responses. In a previous study, we also made a preliminary report that immune responses specific for tumor antigens were enhanced after HCC treatments.[7,10] In addition, we have recently developed a new immunotherapeutic approach for HCC using DC infusion performed during TAE, showing the potential to enhance tumor-specific immune responses.[7]

In the current study, we first attempted to identify the effect of TAE for tumor-specific T-cell responses in patients with HCC. Next, we examined the additional effects of DC infusion to the tumor site after TAE. Finally, we analyzed the relationship between clinical characteristics of patients and T-cell responses after TAE and evaluated whether the activation of tumor-specific T-cell responses can prevent HCC recurrence.

Material and Methods

Patient population

The study examined 33 patients with HCC, consisting of 25 men and 8 women ranging from 48 to 83 years old with a mean age of 66 ± 9 years. Twenty patients were treated by TAE. Thirteen patients were treated by TAE with DC infusion as a part of clinical study, which was approved by ethical committee of Kanazawa University Graduate School of Medical Science and registered in September 2003. The patients who received TAE with DC infusion were selected according to the criteria we previously reported.[7] All subjects were negative for Abs to human immunodeficiency virus (HIV) and gave written informed consent to participate in this study in accordance with the Helsinki declaration.

Treatment of hepatocellular carcinoma

HCCs were detected by imaging modalities such as dynamic CT scan, MR imaging and abdominal arteriography. The diagnosis of HCC was histologically confirmed by taking US-guided needle biopsy specimens, surgical resection or autopsy in 18 cases. For the remaining 15 patients, the diagnosis was based on typical hypervascular tumor staining on angiography in addition to typical findings, which showed hyperattenuated areas in the early phase and hypoattenuation in the late phase on dynamic CT.[33] The tumor size was categorized as "small" (≤2 cm) or "large" (>2 cm), and tumor multiplicity was categorized as "multiple" (≥2 nodules) or "solitary" (single nodule). The TNM stage was classified according to the Union Internationale Contre Le Cancer (UICC) classification system (6th version).[34]

Twenty patients were treated by TAE as previously described.[19,35] In brief, after evaluation of the feeding arteries and surrounding vascular anatomy, a microcatheter (Microferret, Cook, Bloomington, IN) was inserted into the segmental or subsegmental artery with a coaxial method using a 0.016-inch guidewire (Radifocus GT wire, Terumo, Tokyo, Japan). A mixture of the anticancer drug and iodized oil was administered, and the feeding artery was embolized with gelatin sponge particles (Gelfoam; Pharmacia Upjohn, Kalamazoo, MI). The mixture of anticancer drug and iodized oil contained 10–30 mg of Epirubicin (Farmorubicin; Kyowa Hakko Kogyo, Tokyo, Japan), 1–3 ml of iodized oil (Lipiodol Ultra Fluide) and 0.5–1.0 ml of iohexol (Omnipaque 300).

Preparation and injection of autologous DCs

DCs were generated as previously described.[7] In 6 patients, DCs were pulsed with 0.1 KE/ml OK-432 (Chugai Pharmaceutical, Tokyo, Japan), which is a biological response modifier derived from the weakly virulent Su strain of Streptococcus pyogenes,[36,37] for 3 days before injection. The cells were harvested for injection; 5×10^6 cells were reconstituted in 5-ml normal saline containing 1% autologous plasma, mixed with gelatin sponge particles and infused through an arterial catheter following iodized oil injection during TAE.

After TAE or TAE with DC infusion, 26 patients received percutaneous tumor ablation by ethanol injection (PEIT), microwave coagulation (MCT) or radiofrequency (RF). Twenty-one patients were diagnosed with complete necrosis of the tumor lesion using dynamic CT after the completion of treatment. Follow-ups were conducted at outpatient clinics using blood tests and dynamic CT every 3 months for 1 year.

Laboratory and virologic testing

Blood samples were tested for HBsAg and HCVAb by commercial immunoassays (Fuji Rebio, Tokyo, Japan). HLA-based typing of PBMC from patients was performed using complement-dependent microcytotoxicity with HLA typing trays purchased from One Lambda. The serum alpha-fetoprotein (AFP) level was measured by enzyme immunoassay (AxSYM AFP, Abbott Japan, Tokyo, Japan), and the pathological grading of tumor cell differentiation was assessed according to the general rules for the clinical and pathologic study of primary liver cancer.[38] The severity of liver disease (stage of fibrosis) was evaluated according to the criteria of Desmet *et al.*[39]

Interferon-γ enzyme-linked immunospot assay

The prevalence of tumor antigen-specific T cells was determined by interferon (IFN)-γ enzyme-linked immunospot (ELISPOT) analysis (Mabtech, Nacka, Sweden) as previously described.[10,40] HLA-A24-restricted AFP-derived peptides (10 μg/ml), which were AFP_{357} (EYSRRHPQL), AFP_{403} (KYIQESQAL) and AFP_{434} (AYTKKAPQL),[10] and 20 μg/ml AFP derived from human placenta (Morinaga Institute of Biological Science, Yokohama, Japan, purity >98%) were added directly to the wells. These 3 AFP-derived peptides could induce CTLs showing cytotoxicity against hepatoma cells and were frequently recognized by PBMCs of patients with HCC as we previously reported,[10] and therefore, we selected them as an immunogenic peptide. The HLA-A24-restricted AFP and CMV-derived peptides were used only for HLA-A24 or A23 positive patients. Other tumor antigen-derived peptides consisted of $MRP3_{503}$ (LYAWEPSFL), $MRP3_{692}$ (AYVPQQAWI), $MRP3_{765}$ (VYSDADIFL), $hTERT_{167}$ (AYQVCGPPL), $hTERT_{324}$

(VYAETKHFL) and $hTERT_{461}$ (VYGFVRACL), which we previously reported that they were useful for analyzing host immune responses to HCC.[40,41]

PBMCs were added to the wells at 3×10^5 cells/well. In the assay using PBMC depleted $CD4^+$ or $CD8^+$ cells, the number of cells was adjusted to 3×10^5 cells/well after the depletion. Depletion of $CD4^+$ or $CD8^+$ cells was performed by MACS separation system using CD4 or CD8 MicroBeads (Miltenyi Biotec, Auburn, CA) in accordance with the manufacturer's instructions. After the depletion, 1×10^6 cells were stained with CD4 and CD8 antibodies (Becton Dickinson, Tokyo, Japan) and analyzed by FACSCalibur (Becton Dickinson, Tokyo, Japan) to confirm the ratio of $CD4^+$ and $CD8^+$ cells. Data analysis was undertaken with CELLQuest™ software (Becton Dickinson, San Jose, CA).

Plates were analyzed with a KS ELISpot Reader (Zeiss, Tokyo, Japan). The number of specific spots was determined by subtracting the number of spots in the absence of antigen. Responses were considered positive if more than 10 specific spots were detected and if the number of spots in the presence of antigen was at least 2-fold greater than the number of spots in the absence of antigen. Negative controls consisted of incubation of PBMCs with a peptide representing an HLA-A24-restricted epitope derived from HIV envelope protein ($HIVenv_{584}$) and were always <5 spots per 3×10^5 cells.[42] The positive controls consisted of 10 ng/ml phorbol 12-myristate 13-acetate (PMA, Sigma) or a CMV pp65-derived peptide ($CMVpp65_{328}$).[43] All peptides used in this study were synthesized at Sumitomo Pharmaceuticals (Osaka, Japan). ELISPOT analysis was performed before and 2–4 weeks after TAE. In patients receiving additional treatment for complete ablation of tumor, analysis was performed just before the additional treatment. An increase of antigen-specific T cells was defined as significant when T-cell responses changed to positive or if the number of spots detected after TAE was at least 2-fold greater than the number of spots detected before treatment.

Statistical analysis

Unpaired Student's *t*-test was used to analyze the effect of variables on immune responses in patients with HCC. Fisher's exact test (2-sided *p*-value) was used to analyze the frequency of positive immune responses in patients between with TAE and TAE with DC infusion.

Results

T-cell responses to AFP in the patients who received TAE

The frequency of AFP-specific T cells before and after TAE was tested *ex vivo* in an IFN-γ ELISPOT assay. The serum AFP level and number of peripheral lymphocytes and antigen-specific T cells are shown in Table 1. Before treatment, 2 patients showed a specific T-cell response to AFP-derived peptides and 3 patients to protein in 20 patients (Patients 1–20). After treatment, a T-cell response to AFP-derived peptides and protein was detected in 4 and 3 patients, respectively.

When an increase of antigen-specific T cells was defined as significant if T-cell responses changed to positive or the number of spots detected after TAE was at least 2-fold greater than the number of spots detected before treatment, 6 of 20 (30%) patients (Patients 4, 6, 7, 11, 18 and 20) showed a significant increasing of AFP-specific T-cell frequency after treatment. It was observed even in the patient (Patients 6, 7 and 18) who had no T cells specific to corresponding AFP-derived peptides before treatment. When a decrease of antigen-specific T cells was defined as significant if T-cell responses changed from positive to negative or the number of spots detected after TAE was less than half of the number of spots detected before treatment, 4 of 20 (20%) patients (Patients 5, 14, 15 and 16) showed a significant decreasing of AFP-specific T-cell frequency after treatment.

AFP-specific IFN-γ-producing T cells were also analyzed by ELISPOT assay using PBMC depleted $CD4^+$ or $CD8^+$ cells to determine what kind of T cells is responsive to whole AFP. Depletion of $CD4^+$ or $CD8^+$ cells was performed by MACS separation system, and the results were confirmed by flow cytometric analysis (Fig. 1*a*). After depletion of $CD4^+$ or $CD8^+$ cells, the ratio of each cell population was decreased to less than 0.1% of PBMCs. The IFN-γ ELISPOT assay showed that IFN-γ-producing T cells against AFP consisted of both $CD8^+$ and $CD4^+$ cells (Fig. 1*b*).

To confirm the effect of TAE for host immune responses to HCC, we also examined the frequency of tumor antigen-specific T cells in 4 patients (Patients 5, 8, 10 and 14) using MRP3- or hTERT-derived peptides that we previously identified as useful for analyzing host immune responses to HCC.[40,41] A significant increasing of MRP3- or hTERT-specific T-cell frequency was observed in all patients after TAE (Table 2).

T-cell responses to AFP in the patients who received TAE with DC infusion

In 13 patients receiving TAE with DC infusion (Patients 21–33), 2 patients showed a specific T-cell response with AFP-derived peptides and 2 patients with protein before treatment (Table 3). After treatment, 8 patients showed a specific T-cell response to AFP-derived peptides and 3 patients to protein.

Next, we compared TAE with DC infusion with TAE alone regarding the effect to AFP-specific immune response. Table 4 shows the clinical features of patients with HCC who received TAE and TAE with DC infusion and they were not statistically different except liver function.

The frequency of patients who showed both positive and increasing T-cell response with AFP-derived peptides or protein after treatment was significantly higher in patients receiving TAE with DC infusion than in those receiving TAE alone ($p = 0.04$) (Fig. 2*a*). On the other hand, the frequency of patients who showed both positive and increasing T-cell

Table 1. T cell response to AFP and AFP-derived peptides by ELISPOT assay before and after TAE

				Before treatment								After treatment							
Patient	HLA	Additional treatment	Complete ablation	AFP (ng/ml)	Lymph. (μl^{-1})	AFP_{357}	AFP_{403}	AFP_{434}	AFP	$CMVpp65_{328}$	TT	AFP (ng/ml)	Lymph. (μl^{-1})	AFP_{357}	AFP_{403}	AFP_{434}	AFP	$CMVpp65_{328}$	TT
1	A2	RF	C	<10	1,600	ND	ND	ND	1	ND	0	<10	1,400	ND	ND	ND	0	ND	1
2	A26,A31	RF	C	61	1,700	ND	ND	ND	0	ND	**13**	23	900	ND	ND	ND	0	ND	0
3	A11,A26	No	–	100	1,700	ND	ND	ND	5	ND	1	50	1,500	ND	ND	ND	0	ND	0
4	A24	RF	C	18	700	0	7	0	6	0	**25**	16	500	1	**10**	1	1	2	**16**
5	A24,A33	RF	C	2,357	1,200	**13**	2	6	0	**13**	0	700	1,100	2	1	1	0	9	0
6	A24	RF	C	14	1,800	0	0	0	0	0	**42**	<10	1,400	**53**	**27**	**38**	**14**	**36**	**108**
7	A23,A33	No	–	96	500	0	0	0	5	**291**	0	138	800	**46**	0	0	3	**484**	0
8	A24,A26	No	–	142	600	1	0	0	0	0	0	126	500	2	0	0	0	**166**	1
9	A2,A24	RF	C	<10	700	6	1	0	0	9	0	<10	700	0	0	0	0	**32**	**15**
10	A24	PEIT	C	<10	1,300	8	4	8	8	**146**	5	<10	1,300	0	1	1	0	1	1
11	A24,A26	PEIT	N	18	1,100	0	0	0	1	ND	0	13	400	0	0	0	**15**	**10**	**55**
12	A24,A33	RF	N	11	800	3	2	0	4	**94**	**10**	11	700	0	0	0	0	**24**	0
13	A11,A24	PEIT	C	52	1,300	0	2	5	1	2	0	24	1,200	0	0	0	0	0	3
14	A24	RF	C	54	2,400	**25**	5	4	8	**12**	0	67	1,700	0	0	0	0	0	0
15	A2,A24	RF	N	62	1,200	0	3	0	**25**	2	3	14	800	0	0	0	8	0	0
16	A3,A24	RF	C	2,876	900	0	1	0	**13**	0	5	3,285	700	0	0	0	0	0	0
17	A24,A33	No	–	205	400	4	2	3	2	**26**	9	220	100	2	1	0	1	**39**	1
18	A24,A30	RF	C	18	1,100	4	0	3	8	**14**	7	13	900	1	**16**	1	5	**12**	0
19	A2,A24	RF	C	330	1,500	2	0	0	0	**18**	1	36	1,100	0	4	0	3	8	1
20	A2,A33	RF	C	10	1,400	ND	ND	ND	**10**	ND	**68**	<10	800	ND	ND	ND	**31**	ND	**101**

Abbreviations: Lymph., number of lymphocytes; RF, radiofrequency ablation; PEIT, percutaneous ethanol injection therapy; No, no treatment; C, completed; N, not completed; –, not determined; ND, not done. The bold letters show the positive responses in ELISPOT assays.

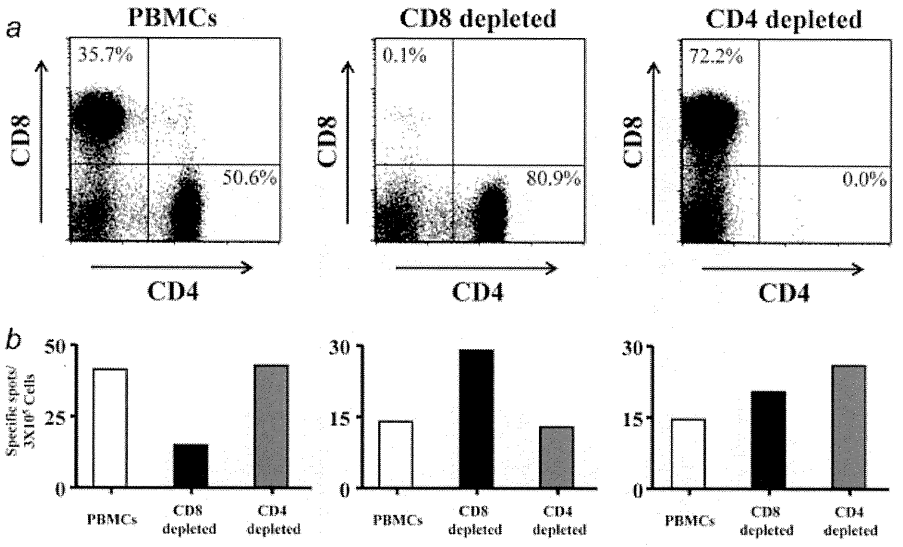

Figure 1. IFN-γ production of CD4- or CD8-depleted T cells against whole AFP. AFP-specific IFN-γ-producing T cells were analyzed by ELISPOT assay using PBMC depleted $CD4^+$ or $CD8^+$ cells to determine what kind of T cells is responsive to whole AFP. Depletion of $CD4^+$ or $CD8^+$ cells was performed by MACS separation system and the results were confirmed by flow cytometric analysis (*a*). IFN-γ ELISPOT assay using nontreated PBMCs and PBMC depleted $CD4^+$ or $CD8^+$ cells showed that T cells producing IFN-γ against whole AFP consisted of both $CD8^+$ and $CD4^+$ cells (*b*). Assays were performed in 5 patients and the representative result is shown.

Table 2. T cell response to other tumor antigen-derived peptides by ELISPOT assay before and after TAE

	Before treatment						After treatment					
Patient	$MRP3_{503}$	$MRP3_{692}$	$MRP3_{765}$	$hTERT_{167}$	$hTERT_{324}$	$hTERT_{461}$	$MRP3_{503}$	$MRP3_{692}$	$MRP3_{765}$	$hTERT_{167}$	$hTERT_{324}$	$hTERT_{461}$
5	2	7	8	0	3.5	7.5	0	0	0	7	3	**35**
8	6	6	1	3	ND	ND	**17**	**18**	**22**	**18**	**14**	9
10	0	1	3	0	5	7	0	4	7	6	**11**	4
14	6	5	0	9	5	**13**	6	14	22	8	**10**	7

Abbreviation: ND, not done. The bold letters show the positive responses in ELISPOT assays.

response with CMV-derived peptide or tetanus toxoid was not different between the 2 groups (Figs. 2*b* and 2*c*).

In the comparison of the mean values of spots generated with AFP-derived peptides, protein, CMV-derived peptides or tetanus toxoid, no significant difference was observed between patients with TAE alone before and after treatment (Figs. 3*a*–3*d*). In contrast, the mean values of spots generated with AFP-derived peptides were significantly higher in patients after TAE with DC infusion than in those before treatment (Fig. 3*e*). The mean values of spots generated with protein, CMV-derived peptides or tetanus toxoid were not significantly different between patients before and after TAE with DC infusion (Figs. 3*f*–3*h*). Based on the above results, we considered that the main difference between TAE alone and TAE with DC infusion was the response to HLA-A24-restricted AFP-derived epitopes. Therefore, to analyze the difference between TAE alone and TAE with DC infusion more precisely, we selected the patients with HLA-A24 or A23 and compared the clinical parameters of both groups. However, there were no statistical differences except liver function in the 2 groups (Table 5).

Enhancement of AFP-specific T-cell responses and treatment outcome

To evaluate the effect of immune enhancement by TAE or TAE with DC infusion for the treatment outcome, we analyzed the clinical course of 17 patients who received complete ablation by additional RFA, PEIT or MCT after these treatments and could be followed up using dynamic CT every 3 months (Table 6). Seven patients showed increasing specific spots for AFP or AFP-derived peptides in ELISPOT assay after TAE. HCC recurrence within 3 months after complete ablation was observed in 3 patients who showed increasing AFP-specific T-cell responses after TAE. Furthermore, recurrence within 6 months after complete ablation was observed

Table 3. T cell response to AFP and AFP-derived peptides by ELISPOT assay before and after TAE with DC infusion

				Before treatment								After treatment							
Patient	HLA	Additional treatment	Complete ablation	AFP (ng/ml)	Lymph. (μl^{-1})	AFP_{357}	AFP_{403}	AFP_{434}	AFP	$CMVpp65_{328}$	TT	AFP (ng/ml)	Lymph. (μl^{-1})	AFP_{357}	AFP_{403}	AFP_{434}	AFP	$CMVpp65_{328}$	TT
21	A24	No	–	332	1,100	7	1	4	ND	**10**	ND	819	800	**11**	0	**10**	ND	**188**	ND
22	A24,A26	RF	N	341	700	0	**26**	5	ND	**68**	ND	237	500	ND	**59**	ND	ND	**81**	ND
23	A11,A24	No	–	41	600	0	2	5	1	2	0	43	400	0	0	0	0	0	3
24	A2,A24	MCT	C	1,260	800	3	8	7	ND	**19**	ND	614	1,300	**26**	4	7	ND	**12**	ND
25	A24,A33	RF	C	11	1,500	0	1	0	**31**	5	**15**	19	900	1	4	**15**	**26**	3	4
26	A24,A33	RF	C	<10	2,000	0	0	0	0	0	0	<10	1,700	0	**16**	0	0	0	0
27	A24,A26	RF	C	16	700	0	0	0	1	1	0	16	700	2	1	**15**	9	0	1
28	A11,A31	RF	N	31	800	ND	ND	ND	3	ND	0	33	700	ND	ND	ND	0	ND	0
29	A11,A33	No	–	<10	1,100	ND	ND	ND	0	ND	0	<10	700	ND	ND	ND	0	ND	1
30	A2,A11	RF	C	13	1,300	ND	ND	ND	8	ND	1	14	1,500	ND	ND	ND	**12**	ND	7
31	A24,A33	RF	C	1,014	800	0	0	0	0	1	0	15	300	0	0	**20**	0	0	0
32	A11,A24	RF	C	<10	1,000	3	3	**11**	**48**	**97**	0	10	1,200	**23**	**20**	**20**	**45**	**91**	**23**
33	A2,A26	RF	C	29	1,300	ND	ND	ND	0	ND	0	27	1,300	ND	ND	ND	0	ND	0

Abbreviations: Lymph., number of lymphocytes; RF, radiofrequency ablation; PEIT, percutaneous ethanol injection therapy; MCT, microwave coagulation therapy; C, completed; N, not completed; –, not determined; ND, not done. The bold letters show the positive responses in ELISPOT assays.

Table 4. Patient characteristics

	Patients treated by TAE (n = 20)	Patients treated by TAE with DC (n = 13)	p-value[1]
Age (years)[2]	66.6 ± 7.8	65.7 ± 10.0	NS
Sex (M/F)	14/6	11/2	NS
HLA (A23 or 24/others)	16/4	9/4	NS
ALT (IU/l)	51.0 ± 47.4	86.9 ± 62.8	NS
Total bilirubin (g/dl)	1.3 ± 0.9	1.5 ± 0.9	NS
Albumin (g/dl)	3.7 ± 0.7	3.2 ± 0.6	NS
AFP level (ng/ml)	322.7 ± 793.0	239.8 ± 418.2	NS
Diff. degrees of HCC (well/moderate or poor/ND[1])	2/6/12	4/4/5	NS
Tumor size (small/large[3])	4/16	1/12	NS
Tumor multiplicity (multiple/solitary)	18/2	12/1	NS
TNM stage (I, II/III, IV)	19/1	11/2	NS
Histology of nontumor liver (LC/chronic hepatitis)	15/5	10/3	NS
Liver function (Child A/B or C)	14/6	3/10	0.02
Etiology (HCV/HBV/others)	12/2/6	13/0/0	NS

[1]Abbreviations: NS, no statistical significance; ND, not determined. [2]Data are expressed as the mean ± SD. [3]Small: ≤2 cm, large: >2 cm.

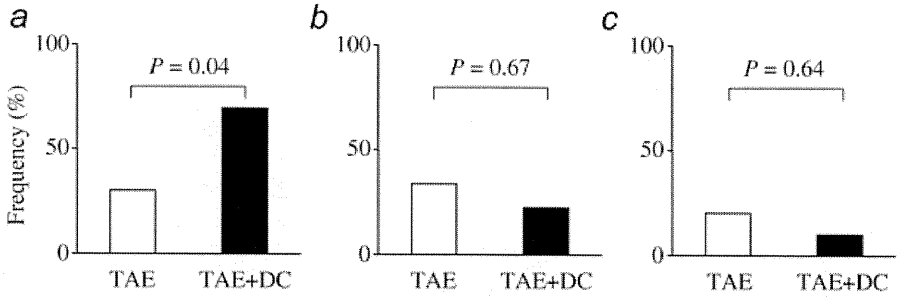

Figure 2. Frequency of the patients who showed enhancement of T-cell responses after treatment. The prevalence of antigen-specific T cells was determined by IFN-γ ELISPOT analysis using alpha-fetoprotein (AFP) and AFP-derived peptides (*a*), CMV pp65-derived peptide (*b*) or tetanus toxoid protein (*c*) in 20 and 13 patients with HCC who received TAE and TAE with DC infusion, respectively.

in 4 and 6 patients who did and did not show increasing AFP-specific T-cell responses, respectively.

Kinetics of AFP-specific T-cell responses before and after TAE

Next, we examined the kinetics of AFP-specific T cells in 8 patients who showed increasing frequency of IFN-γ-producing T cells against AFP or AFP-derived peptides after TAE. The frequency was examined by ELISPOT assay before and 2–4 weeks and 3 months after TAE. Thirteen kinds of AFP-specific T cells showed increasing frequency 2–4 weeks after TAE (Fig. 4); however, the increase was transient and most cell types decreased 3 months after TAE. Three patients showed more than 10 specific spots for AFP or AFP-derived peptides 3 months after TAE (Patients 6, 11 and 30). In analysis of the correlation between the maintenance of AFP-specific T-cell responses and HCC recurrence, 1 patient (Patient 6) had HCC recurrence after 6 months and 1 patient (Patient 30) did not show recurrence. Another patient (Patient 11) did not receive curative ablation and was not analyzed. There was no difference in the kinetics of AFP-specific T cells between patients who received TAE with and without DC infusion.

Discussion

In a previous study, we made a preliminary report that immune responses specific for tumor antigens were enhanced after HCC treatments.[7,10] Similarly, as in our previous or other group's results,[8] we observed enhancement of AFP-specific immune responses in 6 of 20 patients with TAE alone in this study. The enhancement of tumor antigen-specific immune responses was also observed in the cases using MRP3- or hTERT-derived peptides.

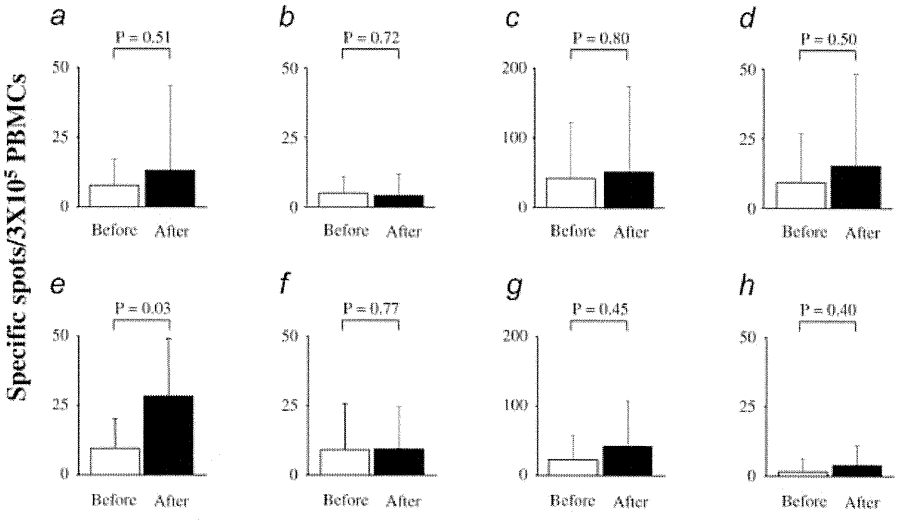

Figure 3. Comparison of direct *ex vivo* analysis (IFN-γ ELISPOT assay) before and after treatment of HCC. The assay was performed using PBMCs of patients who received TAE for AFP-derived peptides (*a*), AFP (*b*), CMV pp65-derived peptide (*c*) or tetanus toxoid protein (*d*). The same assay was performed using PBMCs of patients who received TAE with DC infusion for AFP-derived peptides (*e*), AFP (*f*), CMV pp65-derived peptide (*g*) or tetanus toxoid protein (*h*). AFP and CMV pp65-derived peptides were tested in only HLA-A24 or A23 positive patients. Data are expressed as the mean + SD of specific spots.

Table 5. Characteristics of the patients with HLA-A24 or A23

	Patients treated by TAE (n = 16)	Patients treated by TAE with DC (n = 9)	p-value[1]
Age (years)[2]	65.7 ± 7.8	67.8 ± 10.8	NS
Sex (M/F)	10/6	7/2	NS
ALT (IU/l)	55.9 ± 51.9	75.4 ± 53.0	NS
Total bilirubin (g/dl)	1.4 ± 0.8	1.4 ± 1.1	NS
Albumin (g/dl)	3.6 ± 0.7	3.1 ± 0.6	NS
AFP level (ng/ml)	392.1 ± 877.8	337.2 ± 477.1	NS
Diff. degree of HCC (well/moderate or poor/ND[1])	2/5/9	3/3/3	NS
Tumor size (small/large[3])	3/13	0/9	NS
Tumor multiplicity (multiple/solitary)	15/1	8/1	NS
TNM stage (I, II/III, IV)	15/1	7/2	NS
Histology of nontumor liver (LC/chronic hepatitis)	13/3	8/1	NS
Liver function (Child A/B or C)	10/6	0/9	0.003
Etiology (HCV/HBV/others)	11/1/4	9/0/0	NS

[1]Abbreviations: NS, no statistical significance; ND, not determined. [2]Data are expressed as the mean ± SD. [3]Small: ≤2 cm, large: >2 cm.

The precise mechanism of this phenomenon is still unknown; however, in recent studies, several treatments to destroy tumor cells by necrosis and/or apoptosis have induced antitumor immune responses in animal models[14,44] and even in humans.[6–10] In the study of *in situ* tumor ablation, it is reported that tumor ablation creates a tumor antigen source for the induction of antitumor immunity.[9,44] In another study regarding photodynamic therapy (PDT),[45] it is reported that acute inflammation, expression of heat-shock proteins and providing tumor antigens to DCs caused by PDT induce tumor-specific immune responses.

Based on these results, we hypothesize that DC infusion with TAE can induce antitumor immune responses more effectively than TAE alone. According to DC research in recent years, successful enhancement of the antitumor immune response has been reported by intratumoral

Table 6. Enhancement of AFP-specific T cell response and treatment outcome

	Enhancement of AFP-specific T cell response	Recurrence, 3 months	Recurrence, 6 months
Patient 1	–	N	U
Patient 2	–	N	M
Patient 4	+	M	ND
Patient 5	–	N	M
Patient 6	+	N	U
Patient 9	–	N	M
Patient 10	–	N	N
Patient 13	–	N	N
Patient 14	–	N	N
Patient 16	–	N	M
Patient 19	–	N	U
Patient 24	+	U	ND
Patient 25	+	M	ND
Patient 26	+	N	N
Patient 30	+	N	N
Patient 31	+	N	N
Patient 33	–	N	N

Abbreviations: N, no recurrence; U, uninodular recurrence; M, multinodular recurrence; ND, not determined.

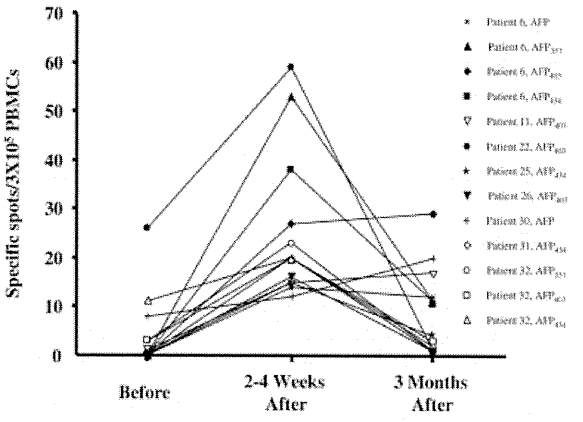

Figure 4. Kinetics of AFP-specific T-cell responses determined by IFN-γ ELISPOT assay before and after TAE. PBMCs were obtained before and 2–4 weeks and 3 months after TAE. Each graph indicates the kinetics of T cells specific for each antigen in each patient. Some patients received additional treatments as indicated in Tables 1 and 3 for a curative treatment after the measurement of T-cell responses at 2–4 weeks after TAE.

administration of DC in combination with tumor ablation.[46,47] Furthermore, immunotherapies using DC have been performed in patients with HCC and their antitumor effects are reported.[48–50] These results support our hypothesis and therefore, in the next step, we examined the immunological effects of DC infusion with TAE.

The comparison of frequency in patients who showed enhancement of AFP-specific immune responses revealed more frequency in patients with DC infusion than in those with TAE alone. On the other hand, there were no differences in the 2 groups in the comparison of frequency for patients who showed enhancement of CMV or TT-specific immune responses. These results suggest that DC infusion with TAE affects tumor-specific immune responses and that the effects are limited to the tumor area.

Some patients with TAE alone showed disappearance of AFP- or control antigen-specific T cells. Although the mechanism of this phenomenon is unknown, anticancer drugs used in TAE might suppress the immune responses, because most of the patients showed decreasing the number of lymphocytes after TAE. These results suggest that TAE alone might give a chance to enhance tumor-specific T-cell responses in only some patients. Further analysis using many more patients with TAE is necessary to make clear the differences in the patients with and without enhancement of T-cell responses. In contrast, disappearance of AFP- or control antigen-specific T cells was not observed in the patients with DC infusion, suggesting strong immunostimulating effect of this treatment.

In analysis of the association between the enhancement of AFP-specific T cells and clinical responses, no correlation could be shown, suggesting that enhancement of T-cell response associated with TAE or TAE with DC infusion may not have protective effect against HCC recurrence. To clarify the mechanism in more detail, we examined the kinetics of AFP-specific T-cell response. Increased frequency of AFP-specific T cells was transient and fell in 4 of 8 patients 3 months after treatment (Fig. 4). Similar to our results, Ayaru *et al.* also reported that the frequency of AFP-specific $CD4^+$ T cells fell in all patients by 1–3 months after TAE.[8] In addition, our results suggest that DC infusion with TAE is not effective to maintain the increased frequency of AFP-specific T cells.

Recent genome profiling studies of HCC show that HCC is a very heterogenous tumor.[51] Furthermore, HCC has multicentric carcinogenesis and develops at different time points. These characters of HCC may also be another reason for no correlation between the enhancement of AFP-specific T cells and clinical responses. The identification of many more tumor antigens and their T-cell epitopes is necessary for more precise analysis of the relationship between antitumor immune response and clinical response, and for immunotherapy.

In the recent study, it is reported that $CD8^+$ T-cell response to AFP is multispecific and AFP-specific IFN-γ-producing $CD8^+$ T cells are directed against different epitopes spreading over the entire AFP sequence with no single

immuno-dominant $CD8^+$ T-cell epitope.[52] Therefore, there is a limitation to our study, because the number of immunogenic AFP-derived peptides applicable in this study is small. However, the results of the present study suggest that TAE with DC infusion enhances the tumor-specific immune responses. Although these modified immune responses may not be sufficient to prevent HCC recurrence because the enhanced immune responses are transient and attenuate within 3 months, these results may contribute to the development of novel immunotherapeutic approach for HCC.

Acknowledgements

The authors thank Ms. Maki Kawamura and Ms. Kazumi Fushimi for technical assistance and for their invaluable help with sample collection.

References

1. Curley SA, Izzo F, Ellis LM, Nicolas Vauthey J, Vallone P. Radiofrequency ablation of hepatocellular cancer in 110 patients with cirrhosis. *Ann Surg* 2000;232: 381–91.
2. Mazzaferro V, Regalia E, Doci R, Andreola S, Pulvirenti A, Bozzetti F, Montalto F, Ammatuna M, Morabito A, Gennari L. Liver transplantation for the treatment of small hepatocellular carcinomas in patients with cirrhosis. *N Engl J Med* 1996;334: 693–9.
3. Urabe T, Kaneko S, Matsushita E, Unoura M, Kobayashi K. Clinical pilot study of intrahepatic arterial chemotherapy with methotrexate, 5-fluorouracil, cisplatin and subcutaneous interferon-alpha-2b for patients with locally advanced hepatocellular carcinoma. *Oncology* 1998; 55:39–47.
4. Ishizaki Y, Kawasaki S. The evolution of liver transplantation for hepatocellular carcinoma (past, present, and future). *J Gastroenterol* 2008;43:18–26.
5. Okuwaki Y, Nakazawa T, Shibuya A, Ono K, Hidaka H, Watanabe M, Kokubu S, Saigenji K. Intrahepatic distant recurrence after radiofrequency ablation for a single small hepatocellular carcinoma: risk factors and patterns. *J Gastroenterol* 2008;43:71–8.
6. Abdel-Hady ES, Martin-Hirsch P, Duggan-Keen M, Stern PL, Moore JV, Corbitt G, Kitchener HC, Hampson IN. Immunological and viral factors associated with the response of vulval intraepithelial neoplasia to photodynamic therapy. *Cancer Res* 2001;61:192–6.
7. Nakamoto Y, Mizukoshi E, Tsuji H, Sakai Y, Kitahara M, Arai K, Yamashita T, Yokoyama K, Mukaida N, Matsushima K, Matsui O, Kaneko S. Combined therapy of transcatheter hepatic arterial embolization with intratumoral dendritic cell infusion for hepatocellular carcinoma: clinical safety. *Clin Exp Immunol* 2007;147: 296–305.
8. Ayaru L, Pereira SP, Alisa A, Pathan AA, Williams R, Davidson B, Burroughs AK, Meyer T, Behboudi S. Unmasking of alpha-fetoprotein-specific CD4(+) T cell responses in hepatocellular carcinoma patients undergoing embolization. *J Immunol* 2007;178:1914–22.
9. Zerbini A, Pilli M, Penna A, Pelosi G, Schianchi C, Molinari A, Schivazappa S, Zibera C, Fagnoni FF, Ferrari C, Missale G. Radiofrequency thermal ablation of hepatocellular carcinoma liver nodules can activate and enhance tumor-specific T-cell responses. *Cancer Res* 2006;66:1139–46.
10. Mizukoshi E, Nakamoto Y, Tsuji H, Yamashita T, Kaneko S. Identification of alpha-fetoprotein-derived peptides recognized by cytotoxic T lymphocytes in HLA-A24+ patients with hepatocellular carcinoma. *Int J Cancer* 2006;118: 1194–204.
11. Gollnick SO, Evans SS, Baumann H, Owczarczak B, Maier P, Vaughan L, Wang WC, Unger E, Henderson BW. Role of cytokines in photodynamic therapy-induced local and systemic inflammation. *Br J Cancer* 2003;88:1772–9.
12. Gollnick SO, Owczarczak B, Maier P. Photodynamic therapy and anti-tumor immunity. *Lasers Surg Med* 2006;38: 509–15.
13. Yamamoto N, Homma S, Sery TW, Donoso LA, Hoober JK. Photodynamic immunopotentiation: in vitro activation of macrophages by treatment of mouse peritoneal cells with haematoporphyrin derivative and light. *Eur J Cancer* 1991;27: 467–71.
14. den Brok MH, Sutmuller RP, van der Voort R, Bennink EJ, Figdor CG, Ruers TJ, Adema GJ. In situ tumor ablation creates an antigen source for the generation of antitumor immunity. *Cancer Res* 2004;64: 4024–9.
15. Kotera Y, Shimizu K, Mule JJ. Comparative analysis of necrotic and apoptotic tumor cells as a source of antigen(s) in dendritic cell-based immunization. *Cancer Res* 2001; 61:8105–9.
16. Sauter B, Albert ML, Francisco L, Larsson M, Somersan S, Bhardwaj N. Consequences of cell death: exposure to necrotic tumor cells, but not primary tissue cells or apoptotic cells, induces the maturation of immunostimulatory dendritic cells. *J Exp Med* 2000;191:423–34.
17. Korbelik M, Sun J, Cecic I. Photodynamic therapy-induced cell surface expression and release of heat shock proteins: relevance for tumor response. *Cancer Res* 2005;65: 1018–26.
18. Takayasu K, Arii S, Ikai I, Omata M, Okita K, Ichida T, Matsuyama Y, Nakanuma Y, Kojiro M, Makuuchi M, Yamaoka Y. Prospective cohort study of transarterial chemoembolization for unresectable hepatocellular carcinoma in 8510 patients. *Gastroenterology* 2006;131:461–9.
19. Matsui O, Kadoya M, Yoshikawa J, Gabata T, Arai K, Demachi H, Miyayama S, Takashima T, Unoura M, Kogayashi K. Small hepatocellular carcinoma: treatment with subsegmental transcatheter arterial embolization. *Radiology* 1993;188:79–83.
20. Yamada R, Kishi K, Sonomura T, Tsuda M, Nomura S, Satoh M. Transcatheter arterial embolization in unresectable hepatocellular carcinoma. *Cardiovasc Intervent Radiol* 1990;13:135–9.
21. Pelletier G, Roche A, Ink O, Anciaux ML, Derhy S, Rougier P, Lenoir C, Attali P, Etienne JP. A randomized trial of hepatic arterial chemoembolization in patients with unresectable hepatocellular carcinoma. *J Hepatol* 1990;11:181–4.
22. Groupe d'Etude et de Traitement du Carcinome Hepatocellulaire. A comparison of lipiodol chemoembolization and conservative treatment for unresectable hepatocellular carcinoma. *N Engl J Med* 1995;332:1256–61.
23. Bruix J, Llovet JM, Castells A, Montana X, Bru C, Ayuso MC, Vilana R, Rodes J. Transarterial embolization versus symptomatic treatment in patients with advanced hepatocellular carcinoma: results of a randomized, controlled trial in a single institution. *Hepatology* 1998;27:1578–83.
24. Llovet JM, Real MI, Montana X, Planas R, Coll S, Aponte J, Ayuso C, Sala M, Muchart J, Sola R, Rodes J, Bruix J. Arterial embolisation or chemoembolisation versus symptomatic treatment in patients with unresectable hepatocellular carcinoma: a randomised controlled trial. *Lancet* 2002;359:1734–9.
25. Lo CM, Ngan H, Tso WK, Liu CL, Lam CM, Poon RT, Fan ST, Wong J. Randomized controlled trial of transarterial lipiodol chemoembolization for unresectable hepatocellular carcinoma. *Hepatology* 2002;35:1164–71.
26. Hsu HC, Wei TC, Tsang YM, Wu MZ, Lin YH, Chuang SM. Histologic assessment of resected hepatocellular carcinoma after

transcatheter hepatic arterial embolization. *Cancer* 1986;57:1184–91.
27. Kenji J, Hyodo I, Tanimizu M, Tanada M, Nishikawa Y, Hosokawa Y, Mandai K, Moriwaki S. Total necrosis of hepatocellular carcinoma with a combination therapy of arterial infusion of chemotherapeutic lipiodol and transcatheter arterial embolization: report of 14 cases. *Semin Oncol* 1997;24: S6–71–S6–80.
28. Kobayashi N, Ishii M, Ueno Y, Kisara N, Chida N, Iwasaki T, Toyota T. Co-expression of Bcl-2 protein and vascular endothelial growth factor in hepatocellular carcinomas treated by chemoembolization. *Liver* 1999;19:25–31.
29. Xiao EH, Li JQ, Huang JF. Effects of p53 on apoptosis and proliferation of hepatocellular carcinoma cells treated with transcatheter arterial chemoembolization. *World J Gastroenterol* 2004;10:190–4.
30. Kanai M, Kohda H, Sekiya C, Namiki M. Effects on interleukin 1 alpha and beta production of peripheral blood mononuclear cells from patients with hepatocellular carcinoma after transcatheter arterial embolization. *Gastroenterol Jpn* 1990;25:662.
31. Yamazaki H, Nishimoto N, Oi H, Matsushita M, Ogata A, Shima Y, Inoue T, Tang JT, Yoshizaki K, Kishimoto T, Inoue T. Serum interleukin 6 as a predicator of the therapeutic effect and adverse reactions after transcatheter arterial embolization. *Cytokine* 1995;7:191–5.
32. Itoh Y, Okanoue T, Ohnishi N, Nishioji K, Sakamoto S, Nagao Y, Nakamura H, Kirishima T, Kashima K. Hepatic damage induced by transcatheter arterial chemoembolization elevates serum concentrations of macrophage-colony stimulating factor. *Liver* 1999;19:97–103.
33. Araki T, Itai Y, Furui S, Tasaka A. Dynamic CT densitometry of hepatic tumors. *AJR Am J Roentgenol* 1980;135: 1037–43.
34. Sobin LH, Wittekind C. TNM classification of malignant tumors, 6th edn. New York: Wiley-Liss, 2002. 81.
35. Terayama N, Miyayama S, Tatsu H, Yamamoto T, Toya D, Tanaka N, Mitsui T, Miura S, Fujisawa M, Kifune K, Matsui O, Takashima T. Subsegmental transcatheter arterial embolization for hepatocellular carcinoma in the caudate lobe. *J Vasc Interv Radiol* 1998;9:501–8.
36. Okamoto H, Shin J, Mion S, Koshimura S, Shimizu R. Studies on the anticancer and streptolysin S-forming abilities of hemolytic streptococci. *Jpn J Microbiol* 1967;11: 323–36.
37. Nakahara S, Tsunoda T, Baba T, Asabe S, Tahara H. Dendritic cells stimulated with a bacterial product, OK-432, efficiently induce cytotoxic T lymphocytes specific to tumor rejection peptide. *Cancer Res* 2003; 63:4112–8.
38. Japan LCSGo. Classification of primary liver cancer. English edn. 2. Tokyo: Kanehara, 1997.
39. Desmet VJ, Gerber M, Hoofnagle JH, Manns M, Scheuer PJ. Classification of chronic hepatitis: diagnosis, grading and staging. *Hepatology* 1994;19:1513–20.
40. Mizukoshi E, Nakamoto Y, Marukawa Y, Arai K, Yamashita T, Tsuji H, Kuzushima K, Takiguchi M, Kaneko S. Cytotoxic T cell responses to human telomerase reverse transcriptase in patients with hepatocellular carcinoma. *Hepatology* 2006;43:1284–94.
41. Mizukoshi E, Honda M, Arai K, Yamashita T, Nakamoto Y, Kaneko S. Expression of multidrug resistance-associated protein 3 and cytotoxic T cell responses in patients with hepatocellular carcinoma. *J Hepatol* 2008;49:946–54.
42. Ikeda-Moore Y, Tomiyama H, Miwa K, Oka S, Iwamoto A, Kaneko Y, Takiguchi M. Identification and characterization of multiple HLA-A24-restricted HIV-1 CTL epitopes: strong epitopes are derived from V regions of HIV-1. *J Immunol* 1997;159: 6242–52.
43. Kuzushima K, Hayashi N, Kimura H, Tsurumi T. Efficient identification of HLA-A*2402-restricted cytomegalovirus-specific CD8(+) T-cell epitopes by a computer algorithm and an enzyme-linked immunospot assay. *Blood* 2001;98:1872–81.
44. Wissniowski TT, Hansler J, Neureiter D, Frieser M, Schaber S, Esslinger B, Voll R, Strobel D, Hahn EG, Schuppan D. Activation of tumor-specific T lymphocytes by radio-frequency ablation of the VX2 hepatoma in rabbits. *Cancer Res* 2003;63: 6496–500.
45. Korbelik M, Krosl G, Krosl J, Dougherty GJ. The role of host lymphoid populations in the response of mouse EMT6 tumor to photodynamic therapy. *Cancer Res* 1996;56: 5647–52.
46. Udagawa M, Kudo-Saito C, Hasegawa G, Yano K, Yamamoto A, Yaguchi M, Toda M, Azuma I, Iwai T, Kawakami Y. Enhancement of immunologic tumor regression by intratumoral administration of dendritic cells in combination with cryoablative tumor pretreatment and Bacillus Calmette-Guerin cell wall skeleton stimulation. *Clin Cancer Res* 2006;12: 7465–75.
47. Machlenkin A, Goldberger O, Tirosh B, Paz A, Volovitz I, Bar-Haim E, Lee SH, Vadai E, Tzehoval E, Eisenbach L. Combined dendritic cell cryotherapy of tumor induces systemic antimetastatic immunity. *Clin Cancer Res* 2005;11: 4955–61.
48. Ladhams A, Schmidt C, Sing G, Butterworth L, Fielding G, Tesar P, Strong R, Leggett B, Powell L, Maddern G, Ellem K, Cooksley G. Treatment of non-resectable hepatocellular carcinoma with autologous tumor-pulsed dendritic cells. *J Gastroenterol Hepatol* 2002;17: 889–96.
49. Iwashita Y, Tahara K, Goto S, Sasaki A, Kai S, Seike M, Chen CL, Kawano K, Kitano S. A phase I study of autologous dendritic cell-based immunotherapy for patients with unresectable primary liver cancer. *Cancer Immunol Immunother* 2003; 52:155–61.
50. Lee WC, Wang HC, Hung CF, Huang PF, Lia CR, Chen MF. Vaccination of advanced hepatocellular carcinoma patients with tumor lysate-pulsed dendritic cells: a clinical trial. *J Immunother* 2005;28: 496–504.
51. Lee JS, Thorgeirsson SS. Genome-scale profiling of gene expression in hepatocellular carcinoma: classification, survival prediction, and identification of therapeutic targets. *Gastroenterology* 2004; 127:S51–5.
52. Thimme R, Neagu M, Boettler T, Neumann-Haefelin C, Kersting N, Geissler M, Makowiec F, Obermaier R, Hopt UT, Blum HE, Spangenberg HC. Comprehensive analysis of the alpha-fetoprotein-specific CD8+ T cell responses in patients with hepatocellular carcinoma. *Hepatology* 2008;48:1821–33.

EpCAM-Positive Hepatocellular Carcinoma Cells Are Tumor-Initiating Cells With Stem/Progenitor Cell Features

TARO YAMASHITA,* JUNFANG JI,* ANURADHA BUDHU,* MARSHONNA FORGUES,* WEN YANG,‡ HONG-YANG WANG,‡ HULIANG JIA,§ QINGHAI YE,§ LUN-XIU QIN,§ ELAINE WAUTHIER,‖ LOLA M. REID,‖ HIROSHI MINATO,¶ MASAO HONDA,¶ SHUICHI KANEKO,¶ ZHAO-YOU TANG,§ and XIN WEI WANG*

*Liver Carcinogenesis Section, Laboratory of Human Carcinogenesis, Center for Cancer Research, National Cancer Institute, Bethesda, Maryland; ‡International Cooperation Laboratory on Signal Transduction, Eastern Hepatobiliary Surgery Institute, Shanghai, China; §Liver Cancer Institute and Zhongshan Hospital, Fudan University, Shanghai, China; ‖Department of Cell and Molecular Physiology, University of North Carolina School of Medicine, Chapel Hill, North Carolina; and the ¶Liver Disease Center and Kanazawa University Hospital, Kanazawa University, Kanazawa, Japan

Background & Aims: **Cancer progression/metastases and embryonic development share many properties including cellular plasticity, dynamic cell motility, and integral interaction with the microenvironment. We hypothesized that the heterogeneous nature of hepatocellular carcinoma (HCC), in part, may be owing to the presence of hepatic cancer cells with stem/progenitor features.** ***Methods:*** **Gene expression profiling and immunohistochemistry analyses were used to analyze 235 tumor specimens derived from 2 recently identified HCC subtypes (EpCAM$^+$ α-fetoprotein [AFP$^+$] HCC and EpCAM$^-$ AFP$^-$ HCC). These subtypes differed in their expression of AFP, a molecule produced in the developing embryo, and EpCAM, a cell surface hepatic stem cell marker. Fluorescence-activated cell sorting was used to isolate EpCAM$^+$ HCC cells, which were tested for hepatic stem/progenitor cell properties.** ***Results:*** **Gene expression and pathway analyses revealed that the EpCAM$^+$ AFP$^+$ HCC subtype had features of hepatic stem/progenitor cells. Indeed, the fluorescence-activated cell sorting–isolated EpCAM$^+$ HCC cells displayed hepatic cancer stem cell–like traits including the abilities to self-renew and differentiate. Moreover, these cells were capable of initiating highly invasive HCC in nonobese diabetic, severe combined immunodeficient mice. Activation of Wnt/β-catenin signaling enriched the EpCAM$^+$ cell population, whereas RNA interference-based blockage of EpCAM, a Wnt/β-catenin signaling target, attenuated the activities of these cells.** ***Conclusions:*** **Taken together, our results suggest that HCC growth and invasiveness is dictated by a subset of EpCAM$^+$ cells, opening a new avenue for HCC cancer cell eradication by targeting Wnt/β-catenin signaling components such as EpCAM.**

Tumors originate from normal cells as a result of accumulated genetic/epigenetic changes. Although considered monoclonal in origin, tumor cells are heterogeneous in their morphology, clinical behavior, and molecular profiles.[1,2] Tumor cell heterogeneity has been explained previously by the clonal evolution model[3]; however, recent evidence has suggested that heterogeneity may be owing to derivation from endogenous stem/progenitor cells[4] or de-differentiation of a transformed cell.[5] This hypothesis supports an early proposal that cancers represent "blocked ontogeny"[6] and a derivative that cancers are transformed stem cells.[7] This renaissance of stem cells as targets of malignant transformation has led to realizations about the similarities between cancer cells and normal stem cells in their capacity to self-renew, produce heterogeneous progenies, and limitlessly divide.[8] The cancer stem cell (CSC) (or tumor-initiating cell) concept is that a subset of cancer cells bear stem cell features that are indispensable for a tumor. Accumulating evidence suggests the involvement of CSCs in the perpetuation of various cancers including leukemia, breast cancer, brain cancer, prostate cancer, and colon cancer.[9–13] Experimentally, putative CSCs have been isolated using cell surface markers specific for normal stem cells. Stem cell–like features of CSC have been confirmed by functional in vitro clonogenicity and in vivo tumorigenicity assays. For example, leukemia-initiating cells in nonobese diabetic, severe combined immunodeficient (NOD/SCID) mice are CD34^{++}CD38$^-$.[11] Breast cancer CSCs are CD44$^+$CD24$^{-/low}$ cells, whereas tumor-initiating cells of the brain, colon, and prostate are CD133$^+$.[10,12,13] CSCs are considered more metastatic and drug-/radiation-resistant than non-CSCs in the tumor, and are responsible for cancer relapse. These findings warrant the development of treatment strategies that can specifically eradicate CSCs.[14,15]

Abbreviations used in this paper: AFP, α-fetoprotein; BIO, 6-bromoindirubin-3′-oxime; CSC, cancer stem cell; FACS, fluorescence-activated cell sorting; 5-FU, 5-fluorouracil; HpSC, hepatic stem cell; IF, immunofluorescence; IHC, immunohistochemistry; MACS, magnetic-activated cell sorting; MeBIO, 1-methyl-BIO; MH, mature hepatocyte; PCNA, proliferating cell nuclear antigen; siRNA, small interfering RNA.

0016-5085/09/$36.00
doi:10.1053/j.gastro.2008.12.004

Hepatocellular carcinoma (HCC) is the third leading cause of cancer death worldwide.[16] Although the cellular origin of HCC is unclear,[17,18] HCC has heterogeneous pathologies and genetic/genomic profiles,[19] suggesting that HCC can initiate in different cell lineages.[20] The liver is considered as a maturational lineage system similar to that in the bone marrow.[21] Experimental evidence indicates that certain forms of hepatic stem cells (HpSCs), present in human livers of all donor ages, are multipotent and can give rise to hepatoblasts,[22,23] which are, in turn, bipotent progenitor cells that can progress either into hepatocytic or biliary lineages.[22,24] α-fetoprotein (AFP) is one of the earliest markers detected in the liver bud specified from the ventral foregut,[25,26] but its expression has been found only in hepatoblasts and to a lesser extent in committed hepatocytic progenitors, not in later lineages or in normal human HpSC.[22] Recent studies also have indicated that EpCAM is a biomarker for HpSC because it is expressed in HpSCs and hepatoblasts.[22-24]

We recently identified a novel HCC classification system based on EpCAM and AFP status.[27] Gene expression profiles revealed that EpCAM$^+$ AFP$^+$ HCC (referred to as *HpSC-HCC*) has progenitor features with poor prognosis, whereas EpCAM$^-$ AFP$^-$ HCC (referred to as *mature hepatocyte-like HCC*; MH-HCC) have adult hepatocyte features with good prognosis. Wnt/β-catenin signaling, a critical player for maintaining embryonic stem cells,[28] is activated in EpCAM$^+$ AFP$^+$ HCC, and EpCAM is a direct transcriptional target of Wnt/β-catenin signaling.[29] Moreover, EpCAM$^+$ AFP$^+$ HCC cells are more sensitive to β-catenin inhibitors than EpCAM$^-$ HCC cells in vitro.[29] Interestingly, a heterogeneous expression of EpCAM and AFP was observed in clinical tissues, a feature that may be attributed to the presence of a subset of CSCs. In this study, we have confirmed that EpCAM$^+$ HCC cells are highly invasive and tumorigenic, and have activated Wnt/β-catenin signaling. We also show a crucial role of EpCAM in the maintenance of hepatic CSCs. Our data shed new light on the pathogenesis of HCC and may open new avenues for therapeutic interventions for targeting hepatic CSCs.

Materials and Methods

Clinical Specimens

HCC samples were obtained with informed consent from patients who underwent radical resection at the Liver Cancer Institute of Fudan University, Eastern Hepatobiliary Surgery Institute, and the Liver Disease Center of Kanazawa University Hospital, and the study was approved by the institutional review boards of the respective institutes. The microarray data from clinical specimens are available publicly (GEO accession number, GSE5975).[27] Array data from a total of 156 HCC cases (155 hepatitis B virus [HBV]-positive) corresponding to 2 subtypes of HCC (ie, HpSC-HCC and MH-HCC), were used to search for HpSC-HCC–associated genes (Supplementary Table 1; see supplementary material online at www.gastrojournal.org). A total of 79 formalin-fixed and paraffin-embedded HCC samples were used for immunohistochemistry (IHC) analyses (Supplementary Table 2; see supplementary material online at www.gastrojournal.org), 56 of which also were used in a recent study.[30] The classification of HpSC-HCC and MH-HCC was based on previously described criteria.[27]

Cell Cultures and Sorting

Human liver cancer cell lines (HuH1 and HuH7) were derived from Health Science Research Resources Bank (JCRB0199 and JCRB0403, respectively) and routinely cultured as previously described.[31] Normal human MHs, provided by the University of Pittsburgh through Liver Tissue Cell Distribution System, were cultured as previously described.[32] Human HpSCs were isolated from fetal livers and cultured in Kubota and Reid's[33] medium as previously described. Wnt10B conditioned medium was prepared as described.[34] Embryonic stem cell culture medium was prepared using Knockout Dulbecco's modified Eagle medium supplemented with 18% of Serum Replacement (Invitrogen, Carlsbad, CA). The pTOP-FLASH and pFOP-FLASH luciferase constructs were described previously.[29] BIO and MeBIO were generous gifts from Ali Brivanlou (The Rockefeller University, New York, NY). For isolating single cell–derived colonies to determine whether heterogeneity is an intrinsic property of EpCAM$^+$ cells, HuH1 and HuH7 cells were resuspended and plated as a single cell per well in 96-well plates. A total of 192 single cells were plated successfully. The clones that grew well were selected 2 weeks after seeding and used for immunofluorescence (IF) analysis. The 5-fluorouracil (5-FU) stock (2 mg/mL; Sigma, St Louis, MO), was prepared in distilled water. Fluorescence-activated cell sorting (FACS) and magnetic-activated cell sorting (MACS) analyses were used to isolate EpCAM$^+$ HCC cells (Supplementary materials; see supplementary Materials and Methods online at www.gastrojournal.org).

Clonogenicity, Spheroid Formation, Invasion, Quantitative Reverse Transcription–Polymerase Chain Reaction, and IHC Assays

For colony formation assays, 2000 EpCAM$^+$ or EpCAM$^-$ cells were seeded in 6-well plates after FACS. After 10 days of culture, cells were fixed by 100% methanol and stained with methylene blue. For spheroid assays, single-cell suspensions of 1000 EpCAM$^+$ or EpCAM$^-$ cells were seeded in 6-well Ultra-Low Attachment Microplates (Corning, Corning, NY) after FACS. The number of spheroids was measured 14 days after seeding. Invasion assays were performed using BD BioCoat Matrigel Matrix Cell Culture Inserts and Control Inserts (BD Biosciences, San Jose, CA) essentially as pre-

viously described.[31] Reverse transcription-polymerase chain reaction and IHC assays are described in detail in the supplementary materials (see supplementary material online at www.gastrojournal.org).

Tumorigenicity in NOD/SCID Mice

Six-week-old NOD/SCID mice (NOD/NCrCRl-*Prkdc*^{scid}) were purchased from Charles River (Charles River Laboratories, Inc, Wilmington, MA). The protocol was approved by the National Cancer Institute-Bethesda Animal Care and Use Committee. Cells were suspended in 200 μL of Dulbecco's modified Eagle medium and Matrigel (1:1), and a subcutaneous injection was performed. The size and incidence of subcutaneous tumors were recorded. For histologic evaluation, tumors were formalin-fixed, paraffin-embedded or embedded directly in OCT compound (Sakura Finetek, Torrance, CA) and stored at −80°C.

RNA Interference

A small interfering RNA (siRNA) specific to *TACSTD1* (SI03019667) and a control siRNA (1022076) were designed and synthesized by Qiagen (Qiagen, Valencia, CA). Transfection was performed using Lipofectamine 2000 (Invitrogen), according to the manufacturer's instructions. A total of 200 nmol/L of siRNA duplex was used for each transfection.

Statistical Analyses

The class comparison and gene clustering analyses were performed as previously described.[30] The canonic pathway analysis was performed using Ingenuity Pathways Analysis (v5.5; Ingenuity Systems, Redwood City, CA). The association of HCC subtypes and clinicopathologic characteristics was examined using either the Mann-Whitney *U* test or the chi-square test. Student *t* tests were used to compare various test groups assayed by colony formation, spheroid formation, or invasion assays. The Kaplan-Meier survival analysis was performed to compare patient survival or tumorigenicity.

Results

A Poor Prognostic HCC Subtype With Molecular Features of HpSC

We re-evaluated the gene expression profiles that were uniquely associated with 2 recently identified prognostic subtypes of HCC (ie, HpSC-HCC and MH-HCC), using a publicly available microarray dataset of 156 HCC cases (GEO accession number: GSE5975). Sixty cases were defined as HpSC-HCC with a poor prognosis and 96 cases were defined as MH-HCC with a good prognosis, based on EpCAM and AFP status.[27] A class-comparison analysis with univariate *t* tests and a global permutation test (1000×) yielded 793 genes that were expressed differentially between HpSC-HCC and MH-HCC ($P < .001$). Hierarchical cluster analyses revealed 2 main gene clusters that were up-regulated (cluster A; 455 genes) or down-regulated (cluster B; 338 genes) in HpSC-HCC (Figure 1*A*). Pathway analysis indicated that the enriched genes in cluster A were associated significantly with known stem cell signaling pathways such as transforming growth factor-β, Wnt/β-catenin, PI3K/Akt, and integrin ($P < .01$) (Figure 1*B*). In contrast, genes in cluster B were associated significantly with mature hepatocyte functions such as xenobiotic metabolism, complement system, and coagulation system ($P < .01$). Noticeably, known HpSC markers such as *KRT19* (CK19), *TACSTD1* (EpCAM), *AFP*, *DKK1*, *DLK1*, and *PROM1* (CD133) were up-regulated significantly in HpSC-HCC, whereas known liver maturation markers such as *UGT2B7* and *CYP3A4* were expressed more abundantly in MH-HCC (Figure 1*C* and Supplementary Tables 3 and 4; see supplementary material online at www.gastrojournal.org). Kaplan-Meier survival analysis revealed that HpSC-HCC patients had a significantly shorter survival than MH-HCC patients ($P = .036$) (Figure 1*D*). Consistently, HpSC-HCC patients had a high frequency of macroscopic and microscopic portal vein invasion (Figure 1*E*).

However, IHC analyses of an additional 79 HCC cases revealed that among 24 HpSC-HCC cases, EpCAM staining was very heterogeneous with a mixture of EpCAM$^+$ and EpCAM$^-$ tumor cells in each tumor (Figure 1*F*, *left panel*). Noticeably, many of the EpCAM$^+$ tumor cells were located at the invasion border zones and often were disseminated at the invasive front (*black arrows*). IF analysis revealed that HCC cells located at the invasive front co-expressed EpCAM, CK19, and AFP (Figure 1*F*, *right panels*). Noticeably, HpSC-HCC patients were significantly younger than MH-HCC patients (Supplementary Tables 1 and 2; see supplementary material online at www.gastrojournal.org). Enrichment of EpCAM$^+$ AFP$^+$ tumor cells at the tumor-invasive front suggested their involvement in HCC invasion and metastasis.

Isolation and Characterization of EpCAM$^+$ Cells in HCC

The results described earlier suggest that HpSC-HCC may be organized in a hierarchical fashion in which EpCAM$^+$ tumor cells act as stem-like cells with an ability to differentiate into EpCAM$^-$ tumor cells. To test this hypothesis, we first evaluated the expression pattern of 7 hepatic stem/maturation markers (EpCAM, CD133, CD90, CK19, Vimentin, Hep-Par1, and β-catenin) in 6 HCC cell lines (Figure 2*A*). All 3 AFP$^+$ cell lines (HuH1, HuH7, and Hep3B) expressed EpCAM, CD133, and cytoplasmic/nuclear β-catenin, whereas the other 3 AFP$^-$ cell lines (SK-Hep-1, HLE, and HLF) did not, consistent with the microarray data. Interestingly, AFP$^+$ cell lines had no CD90$^+$ cell population, which recently was identified as hepatic CSCs,[35] whereas AFP$^-$ cell lines had such a population. Consistent with the IF data, FACS analysis showed that AFP$^+$ cell lines had a subpopulation of

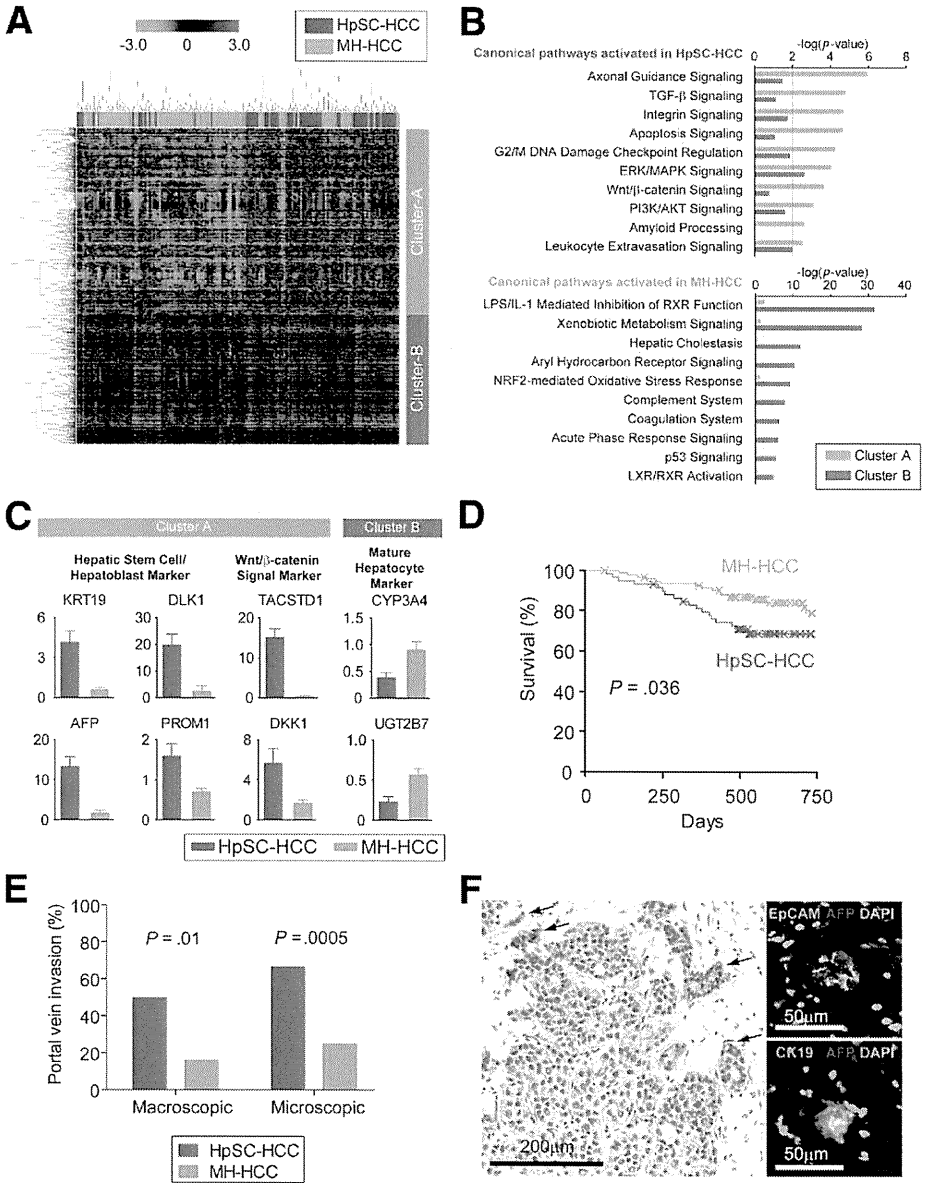

Figure 1. HpSC–HCC represents a subset of invasive HCCs with CSC features. (*A*) Hierarchical cluster analysis based on 793 HpSC–HCC–coregulated genes in 156 HCC cases. Each cell in the matrix represents the expression level of a gene in an individual sample. Red and green cells depict high and low expression levels, respectively, as indicated by the scale bar. (*B*) Pathway analysis of HpSC–HCC–coregulated genes. The top 10 canonical signaling pathways activated in cluster A (*upper panel*) or cluster B (*lower panel*) with statistical significance ($P < .01$) are shown. (*C*) Expression patterns of well-known HpSC and MH markers in each HCC subtype as analyzed by microarray. (*D*) Kaplan–Meier survival analysis of the cases used for array analysis. (*E*) Frequency of macroscopic and microscopic portal vein invasion in HpSC-HCC and MH-HCC used for IHC. (*F*) Representative images of EpCAM, AFP, and CK19 staining in HpSC–HCC samples analyzed by IHC and IF. EpCAM staining illustrates heterogeneous expression of EpCAM in HpSC-HCC (*left panel*). EpCAM$^+$ cells were disseminated in the invasive border (*left panel black arrows*) with expression of AFP (*right top panel*) and CK19 (*right bottom panel*).

EpCAM$^+$ and CD133$^+$, but no CD90$^+$ cells, whereas AFP$^-$ cell lines had a subpopulation of CD90$^+$ cells but no EpCAM$^+$ or CD133$^+$ cells (Figure 2*B*). These data indicate that HpSC-HCC and MH-HCC cell lines have distinct stem cell marker expression patterns, and EpCAM as well as CD133 may be hepatic CSC markers specifically in HpSC-HCC.

We selected 2 human HCC cell lines (HuH1 and HuH7) to isolate EpCAM$^+$ cells because both lines were heterogeneous in EpCAM, AFP, CK19, and β-catenin expression (Figure 2*A* and *B* and Supplementary Figure 1*A*; see supplementary material online at www.gastrojournal.org).[29] We successfully enriched EpCAM$^+$ and EpCAM$^-$ populations from HuH7 cells by FACS, with more than 80% purity in EpCAM$^+$ cells and more than 90% purity in EpCAM$^-$ cells 1 day after sorting (Figure 3*A*). Similar results were obtained when the purity check was performed immediately after sorting (data not shown). EpCAM$^+$ cells also were positive for CK19 and β-catenin (Figure 3*B* and Supplementary Figure 1*B*; see supplementary material online at www.gastrojournal.org) and most were AFP$^+$ (data not shown). In contrast, EpCAM$^-$ cells were negative for these markers but positive for HepPar1, a monoclonal antibody specific to hepatocytes (Figure 3*B*). Consistent with the microarray data described earlier, the levels of *TACSTD1*, *MYC*, and *hTERT* (known HpSC markers) were increased significantly in EpCAM$^+$ HuH7 cells, whereas the levels of *UGT2B7* and *CYP3A4*

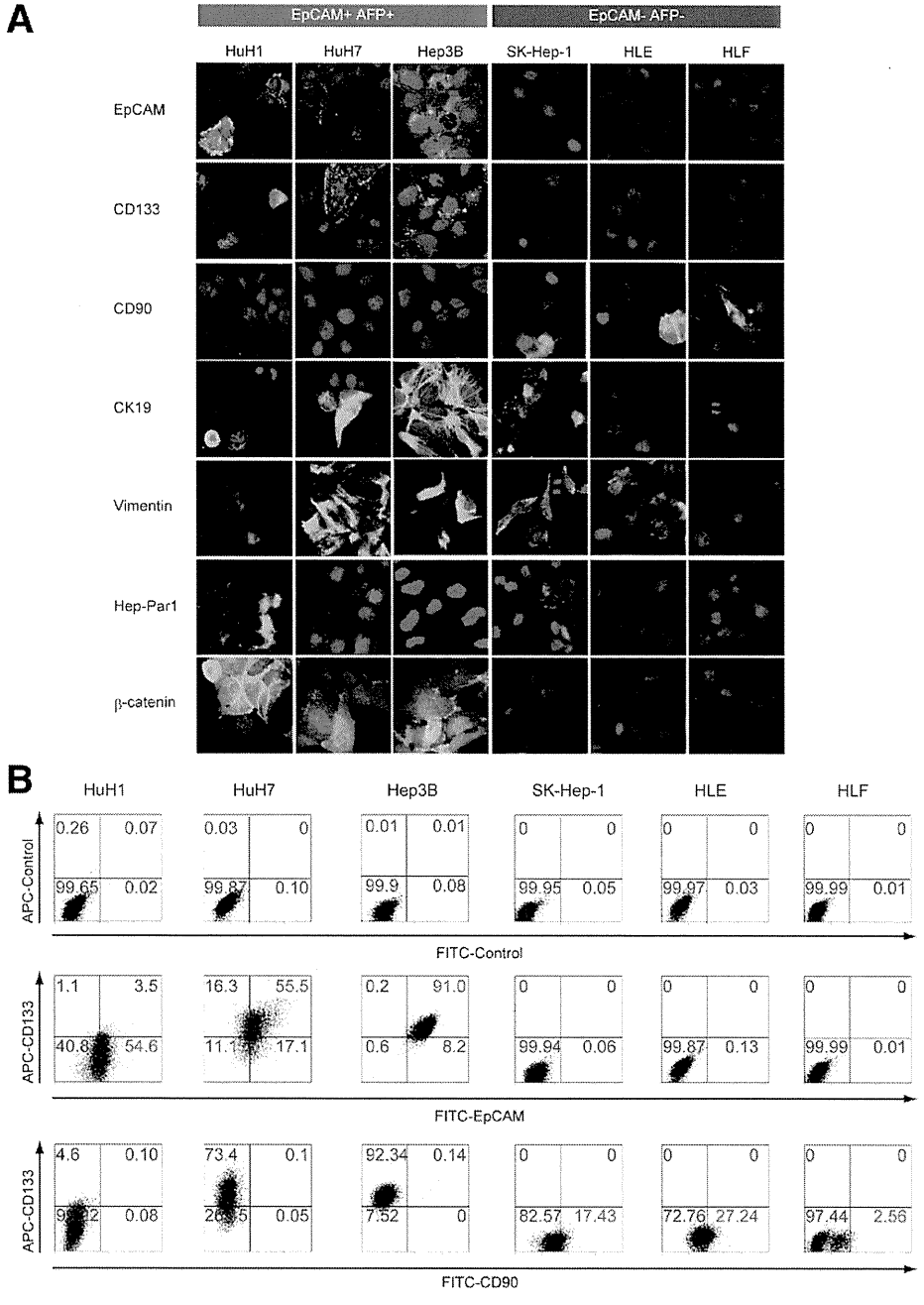

Figure 2. Characterization of hepatic stem cell marker expression in HCC cell lines. (*A*) IF analysis of 6 HCC cell lines (EpCAM$^+$ AFP$^+$ cell lines: HuH1, HuH7, and Hep3B; EpCAM$^-$ AFP$^-$ cell lines: SK-Hep-1, HLE, and HLF) stained with anti-EpCAM, anti-CD133, anti-CD90, anti-CK19, anti-Vimentin, anti-Hep-Par1, and anti-β-catenin antibodies. (*B*) FACS analysis of 6 HCC cell lines stained with anti-EpCAM, anti-CD133, and anti-CD90 antibodies.

(known mature hepatocyte markers) were significantly higher in EpCAM$^-$ HuH7 cells (Figure 3*C*, *left upper panel*). This expression pattern was reminiscent of human HpSC cells (Figure 3*C*, *left lower panel*). Similar results were obtained from HuH1 cells (data not shown). We also compared gene expression patterns of isolated HuH1, HuH7, MH, and HpSC cells using the TaqMan Human Stem Cell Pluripotency Array (Applied Biosystems, Foster City, CA) containing 96 selected human stem cell-related genes. Although a differential expression pattern of stem cell-related genes was evident among HpSC, EpCAM$^+$ HuH1, and EpCAM$^+$ HuH7 cells, the EpCAM$^+$ HCC cells were related more closely to HpSC cells whereas EpCAM$^-$ HCC cells were related more closely to diploid adult mature hepatocytes (Figure 3*C*, *right panel*; and Supplementary Figure 1C; see supplementary material online at www.gastrojournal.org). Thus, it appeared that EpCAM$^+$ HCC cells had a gene expression pattern that is related more closely to HpSC than EpCAM$^-$ HCC cells.

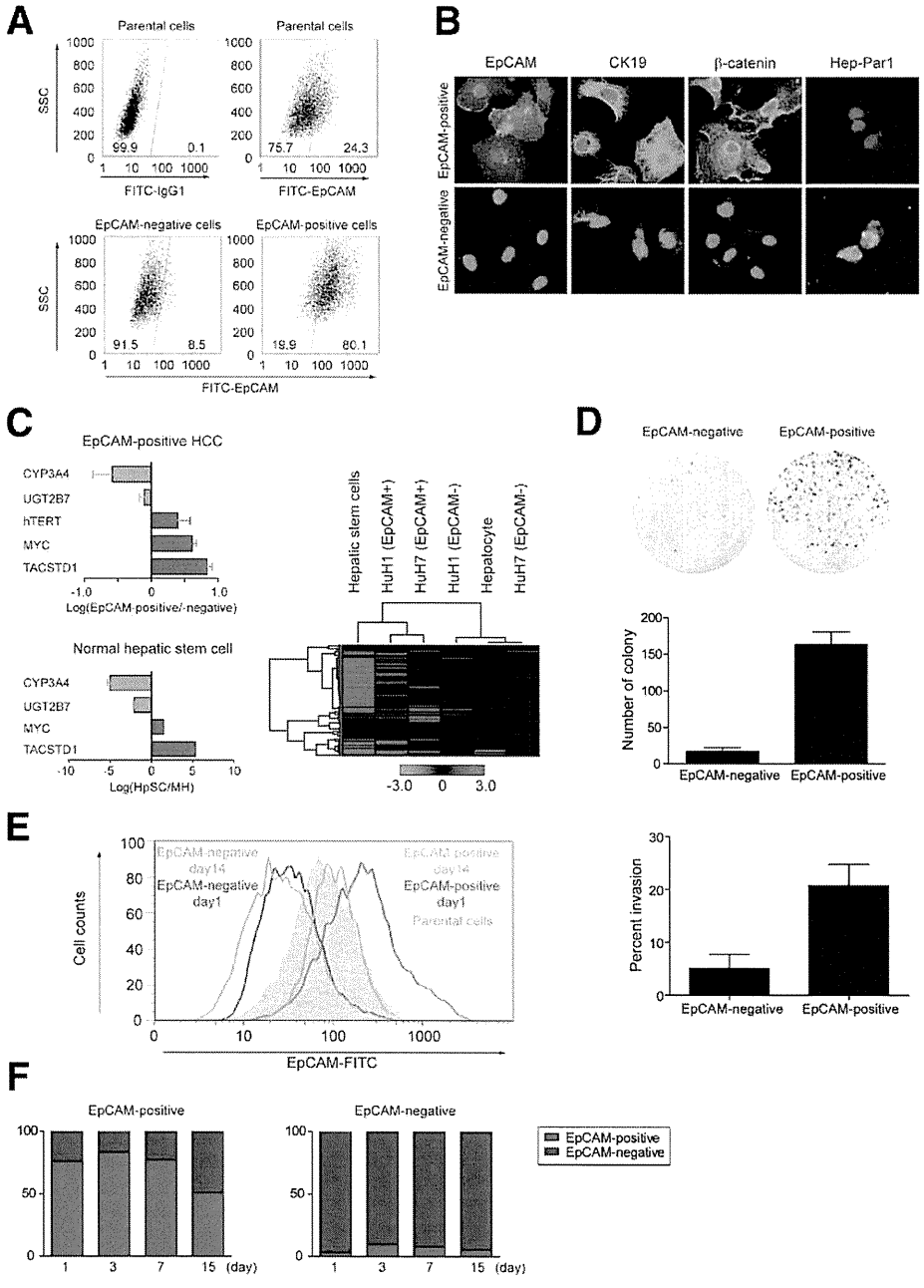

Figure 3. Characterization of EpCAM$^+$ and EpCAM$^-$ cells in HuH7 cells. (*A*) FACS analysis of EpCAM$^+$ and EpCAM$^-$ cells on day 1 after cell sorting. (*B*) IF analysis of cells stained with anti-EpCAM, anti-AFP, anti-CK19, or anti–β-catenin antibodies. (*C*) Quantitative reverse-transcription polymerase chain reaction analysis of EpCAM$^+$ and EpCAM$^-$ HuH7 cells (*left upper panel*) or HpSCs and MHs (*left lower panel*). Experiments were performed in triplicate. Hierarchical cluster analysis of HpSC, MH, and EpCAM$^+$ and EpCAM$^-$ HCC cells using a panel of genes expressed in human embryonic stem cells (*right panel*). Gene expression was measured in quadruplicate. (*D*) Representative photographs of the plates containing colonies derived from 2000 EpCAM$^+$ or EpCAM$^-$ HuH7 cells (*upper panel*). Colony formation experiments were performed in triplicate (mean ± SD) (*middle panel*). Cell invasiveness of EpCAM$^+$ and EpCAM$^-$ cells using the Matrigel invasion assay (*lower panel*). (*E*) Flow cytometer analysis of EpCAM$^+$ and EpCAM$^-$ HuH7 cells stained with anti-EpCAM at days 1 and 14 after cell sorting. (*F*) Percentage of sorted EpCAM$^+$ and EpCAM$^-$ cells after culturing for various times as analyzed by IF. Numbers of EpCAM$^+$ and EpCAM$^-$ cells were counted in 3 independent areas of chamber slides at days 1, 3, 7, and 15 after cell sorting. The average percentages of EpCAM$^+$ or EpCAM$^-$ cells are depicted as *red* or *blue*, respectively.

The isolated EpCAM$^+$ HuH7 cells formed colonies efficiently whereas EpCAM$^-$ cells failed to do so (Figure 3*D*, *upper* and *middle panels*; and Supplementary Figure 2*A* for HuH1 cells; see supplementary material online at www.gastrojournal.org). In addition, EpCAM$^+$ HuH7 cells were much more invasive than EpCAM$^-$ cells ($P <$ .03) (Figure 3*D*, *lower panel*; and Supplementary Figure 2*B* for HuH1 cells; see supplementary material online at www.gastrojournal.org). The EpCAM$^+$ fraction decreased with time in sorted EpCAM$^+$ HuH7 cells from greater than 80% to 50% (Figure 3*E*). However, a small percentage of EpCAM$^+$ cells remained constant in sorted EpCAM$^-$ HuH7 cells. FACS analysis confirmed the results of IF analysis (Figure 3*F* and Supplementary Figure 2*C* for HuH7 and HuH1 cells, respectively; see supplementary material online at www.gastrojournal.org), suggesting that EpCAM$^+$ cells could differentiate into EpCAM$^-$ cells, eventually allowing an enriched EpCAM$^+$ fraction to revert back to parental cells after 14 days of culture. In contrast, EpCAM$^-$ cells maintained their EpCAM$^-$ status. In addition, we successfully isolated 12 HuH1 and 2 HuH7 colonies from 192 single-cell–plated culture wells.

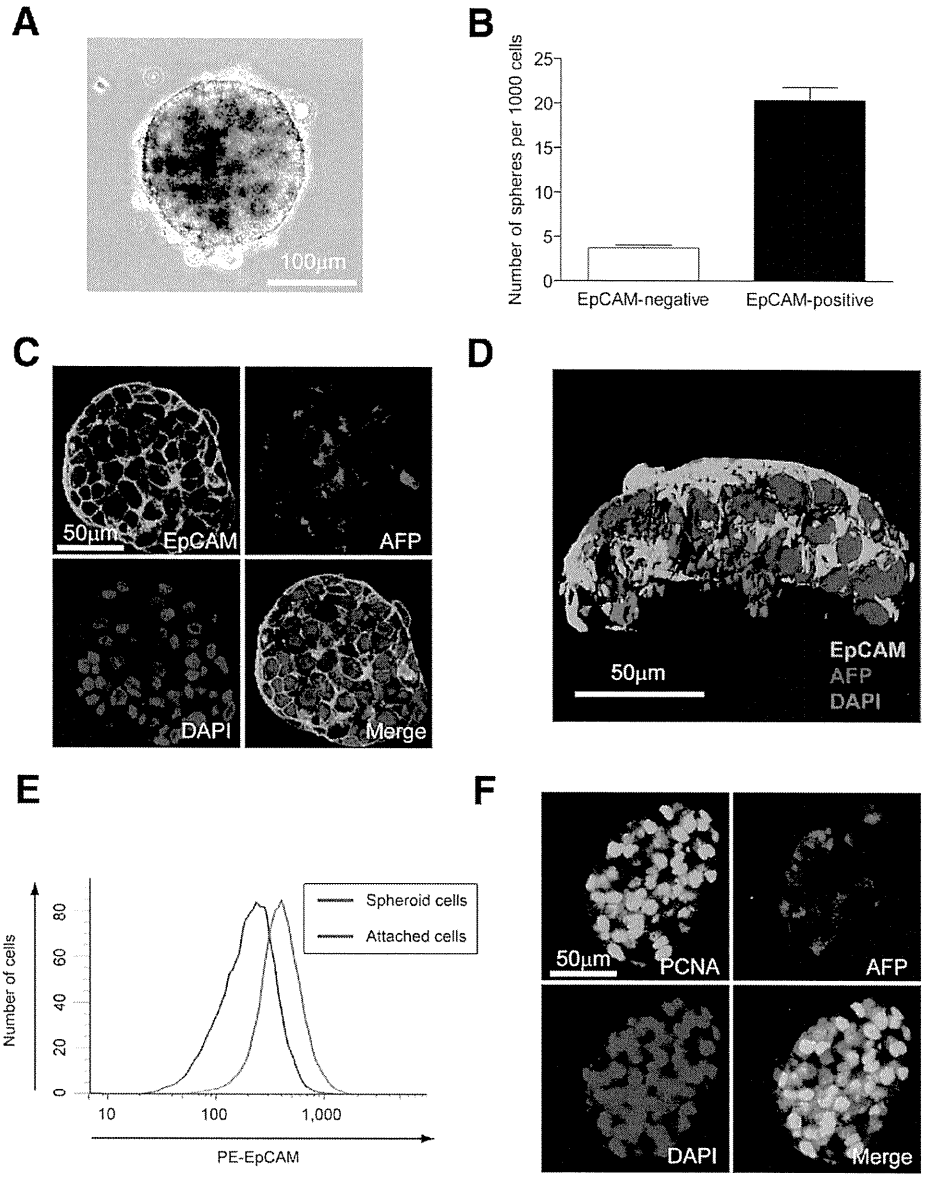

Figure 4. Spheroid formation of EpCAM$^+$ HuH1 HCC cells. (*A*) A representative phase-contrast image of an HCC spheroid derived from an EpCAM$^+$ cell (*scale bar*, 100 μm) and (*B*) total numbers of spheroids from 1000 sorted cells are shown. Experiments were performed in triplicate and data are shown as mean ± SD. (*C*) Representative confocal images of an HCC spheroid co-stained with anti-EpCAM, anti-AFP, and 4′,6-diamidino-2-phenylindole (DAPI) (*scale bar*, 50 μm). (*D*) A 3-dimensional image of an HCC spheroid co-stained with anti-EpCAM, anti-AFP, and DAPI (*scale bar*, 50 μm) reconstructed from confocal images using surface rendering. (*E*) FACS analysis of EpCAM$^+$ cells cultured as spheroid cells (*red*) or attached cells (*blue*) for 14 days after cell sorting. (*F*) Confocal images of an HCC spheroid co-stained with anti-PCNA, anti-AFP, and DAPI (*scale bar*, 50 μm).

However, all colonies were heterogeneous in EpCAM and AFP expression and no colony was completely EpCAM$^-$ (data not shown). Taken together, these results indicate that EpCAM$^+$ HCC cells resemble HpSC features. It appears that EpCAM$^+$ cells, but not EpCAM$^-$ cells, have self-renewal and differentiation capabilities with the ability to form colonies from a single cell, and produce both EpCAM$^+$ and EpCAM$^-$ cells.

It has been shown previously that stem/progenitor cells and cancer stem/progenitor cells can form spheroids in vitro in a nonattached condition.[36,37] Consistently, EpCAM$^+$ cells could form spheroids efficiently, reaching to about 150 to approximately 200 μm in diameter after 14 days of culture (Figure 4*A* and *B*). Interestingly, all cells in a spheroid were EpCAM$^+$, whereas AFP expression was relatively heterogeneous (Figure 4*C* and *D*, and Supplementary movie 1; see supplementary material online at www.gastrojournal.org). Rarely, a few spheroids derived from an EpCAM$^-$ cell fraction were positive for EpCAM (data not shown), suggesting that these spheroids were derived from contaminated residual EpCAM$^+$ cells by FACS sorting. All spheroid cells maintained EpCAM expression while half of the attached cells lost EpCAM expression when the EpCAM$^+$ fraction was cultured for 14 days (Figure 4*E*). Most spheroid cells also abundantly expressed proliferating cell nuclear antigen (PCNA), implying active cell proliferation (Figure 4*F* and Supplementary movie 2; see supplementary material online at www.gastrojournal.org). Thus, a subset of EpCAM$^+$ cells, but not EpCAM$^-$ cells, can form spheroids.

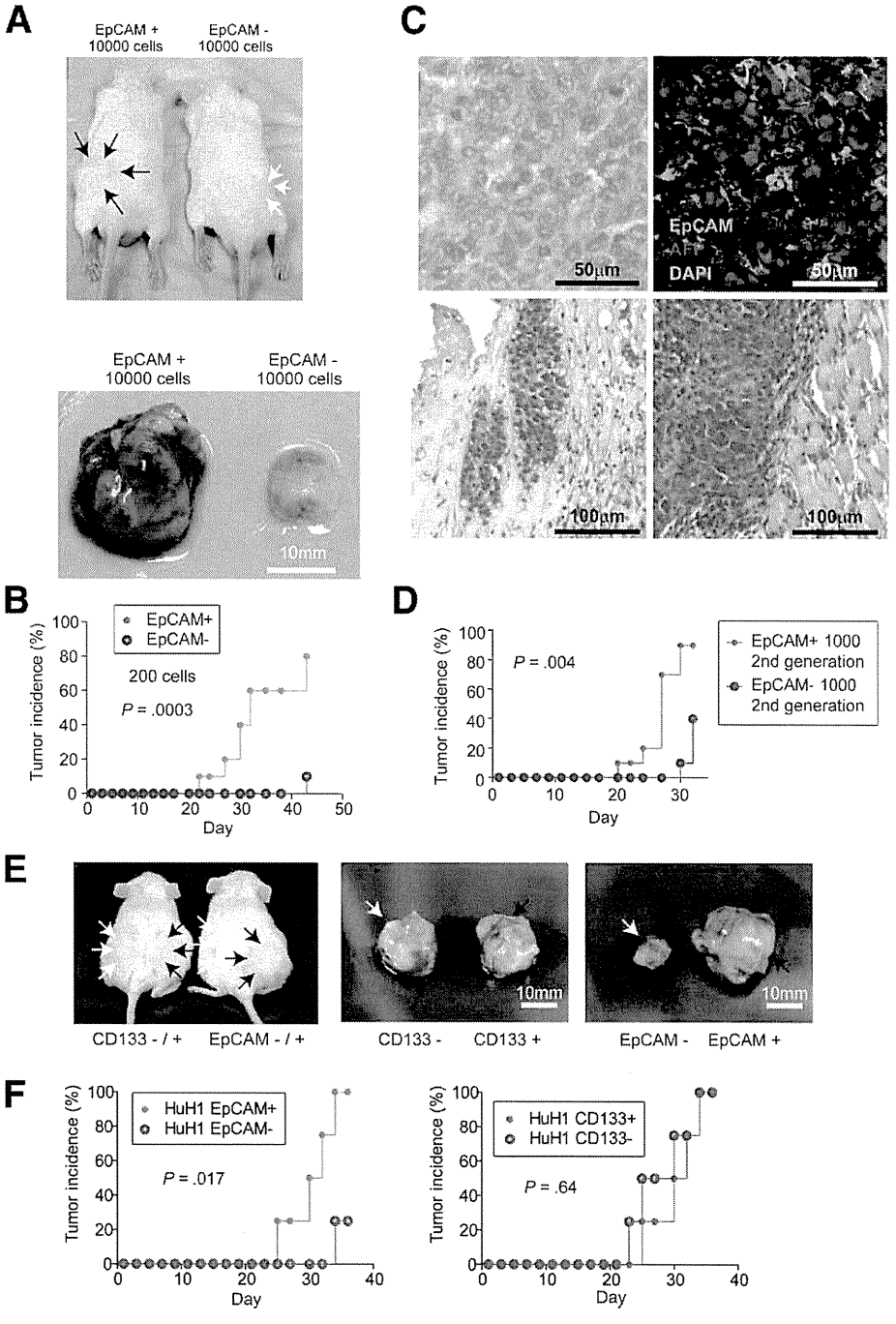

Figure 5. Tumorigenic and invasive potential of EpCAM$^+$ HCC cells. (*A*) Representative NOD/SCID mice (*upper panel*) with subcutaneous tumors (*lower panel*) from EpCAM$^+$ (*black arrows*) or EpCAM$^-$ (*white arrows*) HuH1 cells. (*B*) Tumorigenicity of 200 sorted HuH1 cells. (*C*) Histologic analysis of EpCAM$^+$ HuH1-derived xenografts. H&E staining of a subcutaneous tumor (*left upper panel*) with capsular invasion (*left lower panel*) and muscular invasion (*right lower panel*) and IF of the tumor stained with anti-EpCAM, anti-AFP, and 4′,6-diamidino-2-phenylindole (DAPI) (*right upper panel*) (*scale bar*, 50 μm). (*D*) Tumorigenicity of 1000 sorted cells derived from an EpCAM$^+$ HuH1 xenograft. Data are generated from 10 mice in each group. (*E*) Representative NOD/SCID mice (*left panel*) with subcutaneous tumors from CD133$^+$ (*black arrows*) or CD133$^-$ (*white arrows*) (*middle panel*) and EpCAM$^+$ (black arrows) or EpCAM$^-$ (*white arrows*) (*right panel*) HuH1 cells. (*F*) Tumorigenicity of 1000 HuH1 cells sorted by anti-EpCAM (*left panel*) or anti-CD133 (*right panel*) antibodies.

EpCAM$^+$ HCC Cells as Tumor-Initiating Cells

EpCAM$^+$ HCC cells, but not EpCAM$^-$ HCC cells, could efficiently initiate invasive tumors in NOD/SCID mice (Figure 5). For example, 10,000 EpCAM$^+$ HuH1 cells produced large hypervascular tumors in 100% of mice whereas EpCAM$^-$ cell fractions produced only small and pale-looking tumors in 30% of mice 4 weeks after injection (Figure 5*A* and Supplementary Figure 3*A*; see supplementary material online at www.gastrojournal.org). Similar results were obtained with HuH7 cells (Supplementary Figure 3*B–D*; see supplementary material online at www.gastrojournal.org). As little as 200 EpCAM$^+$ cells could initiate tumors in 8 of 10 injected mice, whereas 200 EpCAM$^-$ cells produced only 1 tumor among 10 injected mice at 6 weeks after transplantation, and the tumor sizes were much larger in the EpCAM$^+$ cells than in the EpCAM$^-$

cells (Figure 5*B* and Supplementary Figure 3*E*; see supplementary material online at www.gastrojournal.org). EpCAM$^+$ cells produced tumors with a mixture of both EpCAM$^+$ and EpCAM$^-$ cells in xenografts, and these cells invaded in the capsule and muscles of the leg adjacent to the tumor (Figure 5*C*). EpCAM$^+$ cells derived from tumors again maintained their tumor-initiating capacity, tumor morphology, and invasive ability in an in vivo serial transplantation experiment (Figure 5*D*). Occasionally, EpCAM$^-$ cell fractions produced a few small tumors that always contained a mixture of EpCAM$^+$ and EpCAM$^-$ cells (data not shown), indicating that the contaminated EpCAM$^+$ cells from FACS sorting contribute to the tumor-initiating ability.

To further validate whether EpCAM$^+$ HCC cells were tumor-initiating cells, we isolated EpCAM$^+$ HCC cells from 2 cases of AFP$^+$ (>600 ng/mL serum AFP) HCC clinical specimens using MACS. Consistently, 1×10^4 EpCAM$^+$ cells could induce tumors in NOD/SCID mice, but up to 1×10^6 EpCAM$^-$ cells failed to do so (Table 1). In addition, similar to HCC cell lines, fresh EpCAM$^+$ tumor cells from 2 clinical HCC specimens were more efficient in forming spheroids in vitro than EpCAM$^-$ cells (Supplementary Figure 4; see supplementary material online at www.gastrojournal.org).

FACS analysis results indicate that a majority of EpCAM$^+$ cells express CD133 in HuH7 cells but not in HuH1 cells (Figure 2*B*), which prompted us to compare the tumorigenic capacity of EpCAM$^+$ and CD133$^+$ cells in these cell lines. Noticeably, EpCAM$^+$ HuH1 cells showed marked tumor-initiating capacity compared with CD133$^+$ HuH1 cells (Figure 5*E* and *F*), whereas EpCAM$^+$ and CD133$^+$ cells had similar tumorigenic ability in HuH7 cells (data not shown).

GSK-3β Inhibition Augments EpCAM$^+$ HCC Cells

To determine the role of Wnt/β-catenin signaling[28] in EpCAM$^+$ HCC cells (Figure 1*B*), we first treated HuH1, HuH7, and HLF cells with a GSK-3β inhibitor BIO (Figure 6*A*), which activates Wnt/β-catenin signaling (Figure 6*B*) and maintains undifferentiation of embryonic stem cells.[38] 6-bromoindirubin-3′-oxime (BIO) increased the EpCAM$^+$ cell population in HuH1 and HuH7 cells when compared with the control methylated BIO (MeBIO) (Figure 6*A*). In contrast, BIO had no effect on the CD90$^+$ cell population, which is more tumorigenic than the CD90$^-$ cell population in HLF (Figure 6*A* and data not shown). Enrichment of EpCAM$^+$ cells was provoked further by the treatment of Wnt10B-conditioned media in HuH7 cells (Figure 6*C*).[34] BIO induced morphologic alteration of HuH7 cells because most cells became small and round when compared with MeBIO and suppressed EpCAM$^-$ AFP$^-$ cell populations (Figure 6*D*). Moreover, BIO induced *TACSTD1*, *MYC*, and *hTERT* expression and spheroid formation (Figure 6*E* and *F*).

Table 1. The Tumor-Initiating Capacity of EpCAM$^+$ Cells From Clinical HCC Specimens

HCC patients				Tumor incidence (mice with tumors/total no. of mice injected)	
No.	% of EpCAM$^+$ HCC cells	Groups	No. of cells injected	2 months	3 months
1	5.2	EpCAM$^+$	1×10^3	0/3	0/3
			1×10^4	2/3	2/3
			1×10^5	2/2	2/2
		EpCAM$^-$	1×10^5	0/3	0/3
			1×10^6	0/2	0/2
2	1.4	EpCAM$^+$	1×10^3	0/2	0/2
			1×10^4	0/1	1/1
		EpCAM$^-$	1×10^4	0/3	0/3
			1×10^5	0/2	0/2

EpCAM Blockage by RNA Interference

One of the hallmarks of CSCs is its resistance to conventional chemotherapeutic agents resulting in tumor relapse and thus targeting CSCs is critical to achieve successful tumor remission. Consistently, 5-FU could increase the EpCAM$^+$ population and spheroid formation of HuH1 and HuH7 cells (Figure 7*A* and *B*) (data not shown), suggesting a differential sensitivity of EpCAM$^+$ and EpCAM$^-$ HCC cells to 5-FU. In contrast, EpCAM blockage via RNA interference dramatically decreased the population of EpCAM$^+$ cells (Figure 7*C*), and significantly inhibited cellular invasion, spheroid formation, and tumorigenicity of HuH1 cells (Figure 7*D–F*). Thus, EpCAM may serve as a molecular target to eliminate HCC cells with stem/progenitor cell features.

Discussion

The cellular origin of HCC is currently in debate. In this study, we found that EpCAM can serve as a marker to enrich HCC cells with tumor-initiating ability and with some stem/progenitor cell traits. EpCAM is expressed in many human cancers with an epithelial origin.[39] During embryogenesis, EpCAM is expressed in fertilized oocytes, embryonic stem cells, and embryoid bodies, suggesting its role in early stage embryogenesis.[40] Furthermore, a recent article indicated that EpCAM is expressed in colonic and breast CSCs.[41] Taken together, these data suggest a critical role of EpCAM in CSCs as well as embryonic and somatic stem cells. Consistently, we found that EpCAM expression is regulated by Wnt/β-catenin signaling[29] and tumorigenic and highly invasive HpSC-HCC is orchestrated by a subset of cells expressing EpCAM and AFP with stem cell–like features and self-renewal and differentiation capabilities regulated by Wnt/β-catenin signaling (this study). Thus, EpCAM may be a common gene expressed in undifferentiated normal cells and HCCs with activated Wnt/β-catenin signaling. It may act as a downstream molecule

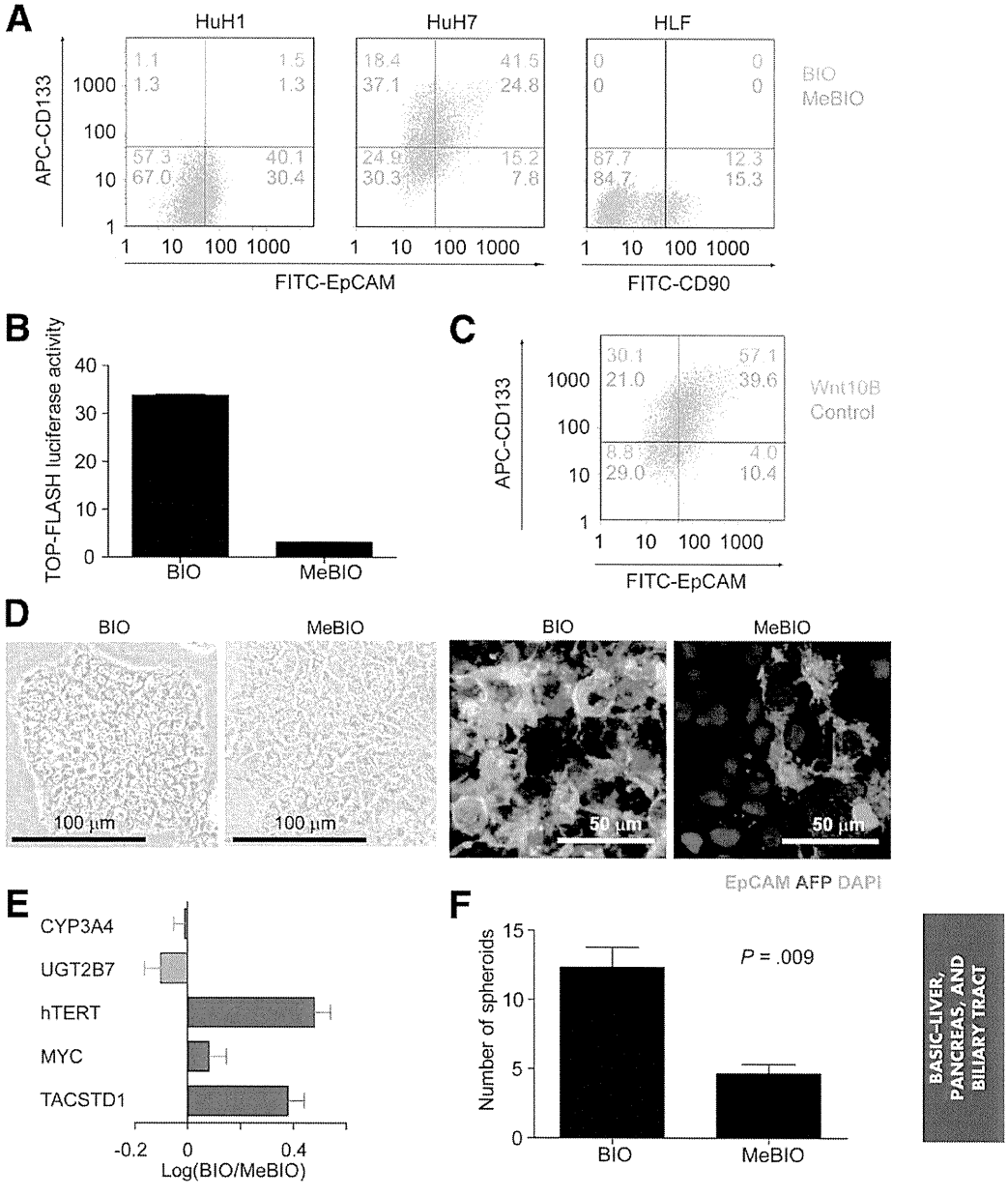

Figure 6. Wnt/β-catenin signaling augments EpCAM$^+$ HCC cells. (*A*) Flow cytometer analysis of HuH1, HuH7, and HLF cells treated with 2 μmol/L of BIO (*orange*) or MeBIO (*green*) for 10 days and stained with anti-EpCAM, anti-CD133 and anti-CD90 antibodies. (*B*) TOP-FLASH luciferase assays of HuH7 cells treated with 2 μmol/L of BIO or MeBIO. (*C*) Flow cytometer analysis of HuH7 cells cultured in normal media (Dulbecco's modified Eagle medium supplemented with 10% FBS) or Wnt10B conditioned media (details are described in the Materials and Methods section). Cells were cultured in each medium for 2 weeks. (*D*) Representative phase-contrast images (*left panel*: *scale bar*, 100 μm) or IF images (*right panel*: *scale bar*, 50 μm) of HuH7 cells treated with 2 μmol/L of BIO or MeBIO for 14 days. (*E*) Quantitative reverse transcription-polymerase chain reaction analysis of representative HpSC-HCC–related genes in HuH7 cells treated with 2 μmol/L of BIO or MeBIO for 14 days. (*F*) Spheroid formation assay of HuH7 cells treated with 2 μmol/L of BIO or MeBIO for 14 days (mean ± SD). FITC, fluorescein isothiocyanate.

to maintain HCC stemness and serve as a good marker for HCC initiating cells.

CD133 or CD90 have been used to identify potential hepatic CSCs.[35,42] CD133 is expressed in normal and malignant stem cells of the neural, hematopoietic, epithelial, hepatic, and endothelial lineages,[23,43,44] suggesting that CD133 is also a common marker to detect normal cells and CSCs. Captivatingly, EpCAM expression overlaps with CD133 expression in normal human colon tissues and colorectal cancer tissues, yet CD133$^+$ and CD133$^-$ cells are equally tumorigenic.[45] Similarly, we found that EpCAM$^+$ and EpCAM$^-$ HuH1 cells equally expressed CD133, but only EpCAM$^+$ cells developed large hypervascular tumors. Our data suggest that EpCAM may be a better marker than CD133 to enrich HCC tumor-initiating cells from AFP$^+$ tumors. We also found that CD90 expression was limited to HCC cell lines that are EpCAM$^-$ AFP$^-$, and Wnt/β-catenin signaling had little effect on CD90$^+$ cell enrichment. These results suggest that the expression patterns of various stem cell markers in tumor-initiating cells with stem/progenitor cell features may be different in each HCC subtype, possibly owing to the heterogeneity of activated signaling pathways in normal stem/progenitor cells where these tumor-initiating cells may originate. Therefore, it would be useful to